Ph.D. Dissertation

Structure Activity Study on hA5G18 Peptide (DDFVFYVGGYPS) from Laminin α5 Chain for Amyloid-like Fibril Formation and Cell Adhesion

January / 2023

Guangrui Zhang

TABLE OF CONTENTS

ABBREVIATION

BSA: bovine serum albumin
CNBr: cyanogen bromide
DIC: *N, N*'-diisopropylcarbodiimide
DMEM: Dulbecco's modified Eagle's medium
DMF: *N, N*-dimethylformamide
EDTA: ethylenediaminetetraacetic acid
ECM: extracellular matrix
FBS: fetal bovine serum
Fmoc: (9-fluorenyl)-methoxycarbonyl
G domain: globular domain
HDF: human neonatal dermal fibroblast
HOBt: 1-hydroybenzotriazole
hr: hour
HPLC: high performance liquid chromatography
HSPG: heparin sulfate proteoglycan
LG module: laminin globular module
MS: mass spectrometory
Milli-Q: simply water purified using a Millipore Milli-Q lab water system
min: minute
PBS: phosphate-buffered saline
S.D.: standard deviation
TEM: transmission electron microscope
TFA: trifluoroacetic acid
UV: ultraviolet

Amino acid
Ala (A): alanine
Cys (C): cysteine
Asp (D): aspartic acid
Glu (E): glutamic acid
Phe (F): phenylalanine
Gly (G): glycine
His (H): histidine

Ile (I): isoleucine
Lys (K): lysine
Leu (L): leucine
Met (M): methionine
Asn (N): asparagine
Pro (P): proline
Gln (Q): glutamine
Arg (R): arginine
Ser (S): serine
Thr (T): threonine
Val (V): valine
Trp (T): tryptophan
Tyr (Y): tyrosine

PROLOGUE

Basement membranes are a thin extracellular matrix (ECM) underlying epithelia and endothelia and surrounding muscle, adipose, and peripheral nerve cells. Basement membranes, consisting of laminins, type IV collagen, perlecan, and nidogens, are complex and precise supramolecular architectures. It has been reported that these components bind together to form a matrix, which provides structural support for tissues and has various biological activities such as tissue repair, tumor growth and metastasis, and wound healing [1, 2]. Among the basement membrane components, laminins play a critical role for the biological activities.

Laminin is a heterotrimeric glycoprotein with a cruciform structure composed of three subunits: α, β, and γ chains (**Figure 1**) [3-5]. Laminin has multiple biological activities, such as cell adhesion, cell migration, angiogenesis, and neurite outgrowth, and it plays a critical role in the basement membrane function [6]. To date, five α chains (α1-α5), three β chains (β1-β3), and three γ chains (γ1-γ3) have been identified and at least 19 different laminin isoforms have been discovered by various combination of each subunit. The α chains play a vital role of the diverse biological functions of laminins and localize in a tissue- and developmental stage-specific manner [5].

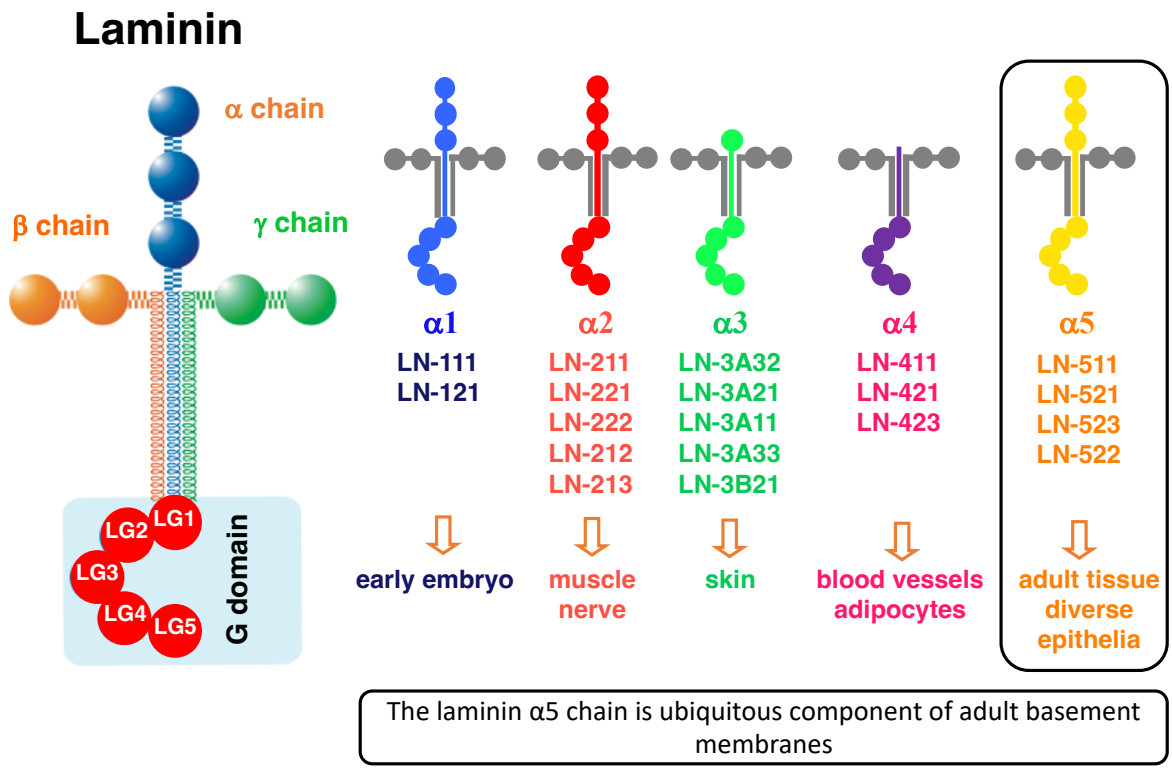

Figure 1. Laminin isoforms.

In recent years, studies on the synthesis of disaggregated fragments, recombinant proteins, and recombinant peptides have shown that various biological activities originate from different active sequences of the laminin molecule. The active peptides specifically interact with cellular receptors, including integrins and syndecan, a membrane-associated heparin sulfate proteoglycan (HSPG) [7-9], and are useful to understand the biological function of laminins and to apply for biomaterials and drug delivery systems [10,11].

Mouse laminin-111 (α1β1γ1) is an earlier discovered isoform of laminin. Nomizu et al. have identified many biologically active sequences by a systematic screening using 673 synthetic peptides covered the entire amino acid sequence of mouse laminin-111 [9,12-15]. Many of the active peptides exhibit cell- and/or receptor-specific activities. [9,12-15]. The biologically active sequences are reported to be abundant in the globular domain, which named as G domain, located at the C-terminus of the laminin α chains [16]. The G domain comprises 5 laminin globular modules (LG1-LG5 modules), each consisting of approximately 200 amino acid residues, and plays an essential role in interacting with cells or other ECM constituent molecules [17]. For example, AG73 (RKRLQVQLSIRT, mouse laminin α1 chain, 2719-2730), located in the LG4 module, specifically binds to syndecans, and promotes cell adhesion, neurite outgrowth, angiogenesis, and wound healing [18-21]. In addition, EF1 (ATLQLQEGRLHFMDFLGKR, mouse laminin α1 chain, 2749-2767), located in the LG4 module, promotes α2β1 integrin-mediated cell attachment and spreading [22,23]. AG73 and EF1 specifically inhibited the cell attachment to a recombinant laminin α1 chain LG4-5 modules [22,23]. These results suggest that the laminin α chain G domain plays an essential role in the biological activity of laminin molecules.

Previously, Kumai et al. screened biologically active sequences in the human laminin α5 chain G domain using 113 synthetic peptides by a peptide-coated plate and peptide-conjugated chitosan matrix assays [27]. Seventeen active peptides were identified in the peptide-coated plate and/or peptide-conjugated chitosan matrix assays. Three peptides, hA5G18 (DDFVFYVGGYPS), hA5G26 (LDGTGFARISFD), and hA5G74 (GSLSSHLEFVGI), promoted integrin β1-mediated cell spreading. hA5G74 promoted cell attachment and spreading in both assays, but hA5G18 and hA5G26 showed activity only in the peptide-coated plate assay. These results suggested that hA5G18 and hA5G26 aggregate on the plastic plates and promote cell adhesion, but the mechanism of the aggregation has not been identified.

Amyloid fibrils are a general term for fibrous insoluble polypeptides or proteins with overlapping β-sheet configurations. Although the molecular size of amyloid fibrils is relatively small, it has a well-defined structure and properties that other proteins do not have. Various proteins form amyloid fibrils, including amyloid β protein, produced after the enzymatic

cleavage of amyloid precursor protein, transthyretin, insulin, and lysozyme. They are unrelated and do not share structural or sequence similarities. These proteins usually have important biological functions in the human body. Once these proteins form amyloid fibrils and accumulate, not only the original function will be destroyed, but also the amyloid fibrils cause various diseases. Amyloid fibril aggregation is closely related to many diseases, such as Alzheimer's disease, type II diabetes, Parkinson's disease, prion diseases, and systemic polyneuropathies [28-31]. Detailed studies have also been conducted on the structural characteristics of amyloid β oligomers and fibrils in the neural tissue of Alzheimer's disease. Differences in morphology, physicochemical properties, and cytotoxicity occur due to their structural diversity [32].

However, while all of these proteins folded differently than normal proteins, the same structure was always found at the core of the fibrils. This unique structure may be due to the substantial charges carried by the constituent parts of the fibrils. Especially their cross-beta-sheet quaternary structure. Individual proteins build long filaments that link side by side into ribbons. These stacks of tightly hydrogen-bonded β-sheets are perpendicular to the long axis of the fibril. And when we viewed with an electron microscope, these fibrils have a straight, unbranched character. They typically bind specifically using fluorescent dyes such as Congo red and Thioflavin T [33,34]. Alternatively, they can be identified indirectly using dye polarimetry, circular dichroism, or Fourier transform infrared spectroscopy. Previously, diverse amyloidogenic peptides were identified from laminin sequences [35,36]. These peptides were stained with Congo red, and most of the peptides showed amyloid-like fibril formation in transmission electron microscope (TEM) analysis.

Many of the amyloidogenic peptides contained basic amino acids, and their cellular effects, including promotion of cell attachment and spreading and neurite outgrowth, have been described. [35]. The amyloidogenic peptides are useful to understand the effect of the degraded proteins *in vivo*. Further, amyloidogenic peptides have been modified with biologically active peptides and applied for multifunctional biomaterials [37]. Amyloidogenic peptides are useful to understand the function of degraded proteins and to use for biomaterials.

In chapter 1, amyloidogenic peptides were identified from the human α5 chain G domain peptides. Active core sequences of the amyloidogenic peptides for the cell attachment and amyloid-like fibril formation were identified. In chapter 2, functional biomaterials for cell scaffold were developed using an active core sequence of the amyloidogenic peptide FVFYV and cell adhesive peptides.

Chapter 1: Identification of amyloidogenic peptides from the human α5 chain G domain

1. Introduction

The laminin α5 chain is composed of laminin-511 (α5β1γ1), laminin-521 (α5β2γ1), laminin-522 (α5β2γ2), and laminin-523 (α5β2γ3) and ubiquitously locates as a basement membrane component (Figure 1) [25]. Laminin α5 chain deficiency has been reported to affect mouse developmental stages such as neural tube obstruction, placenta formation, glomerulogenesis, and intestinal smooth muscle [38-42]. In addition, the laminin α5 chain interacts with integrin receptors such as integrin α3β1 and α6β1 and non-integrin receptors such as syndecan, α-dystroglycan, and Lutheran/basal cell adhesion molecule and plays an essential role in development [43-47].

Previously, Kumai et al. screened biologically active sequences in the human laminin α5 chain G domain using 113 synthetic peptides by peptide-coated plate and peptide-conjugated chitosan matrix assays [27]. In this screening, 17 peptides showed cell attachment activity in both or either peptide-coated plated and/or peptide-conjugated chitosan matrix assays, and 3 peptides, hA5G18 (DDFVFYVGGYPS), hA5G26 (LDGTGFARISFD), and hA5G74 (GSLSSHLEFVGI), promoted integrin β1 mediated cell spreading. The hA5G74 peptide promoted cell attachment and spreading in both assays. In contrast, hA5G18 and hA5G26 showed cell attachment activity only in the peptide-coated plated assay. These results suggested that hA5G18 and hA5G26 aggregate on the plastic plates and promote cell attachment, but mechanism of the aggregation has not been identified.

In this Chapter, I focus on the hA5G18 and hA5G26 peptides and examine their amyloidogenicity and biological activity.

2. Results and Discussion

2.1. Identification of amyloidogenic peptides from the human laminin α5 chain G domain

The hA5G18 and hA5G26 peptides, derived from the human laminin α5 chain G domain, promoted integrin-mediated cell attachment and spreading only in a peptide-coated plated assay [27]. I focused on hA5G18 and hA5G26 and evaluated their amyloidogenicity using Congo red assay and TEM analysis (**Figure 2**). B133 (DSITKYFQMSLE), an amyloidogenic peptide derived from the laminin β1 chain and promotes integrin-mediated cell adhesion, was used as a positive control [36, 49].

First, effect of the peptides on the Congo red absorption spectrum was evaluated (**Figure 2A**). Congo red binds to amyloid fibrils and promotes an absorption peak shift from 490 to 540 nm. The Congo red absorption peak at 490 nm was significantly shifted at 540 nm by hA5G18 similar to that by B133 but was not influenced by hA5G26. These results suggest that hA5G18 is amyloidogenic but hA5G26 is not.

Amyloid-like fibrils are 7-10 nm insoluble fibrils with a cross-sheet structure. I examined the fibril formation of the peptides using TEM (**Figure 2B**). hA5G18 exhibited typical amyloid-like fibrils similar to that of B133, but hA5G26 did not form fibrils. These results indicate that hA5G18 forms amyloid-like fibrils.

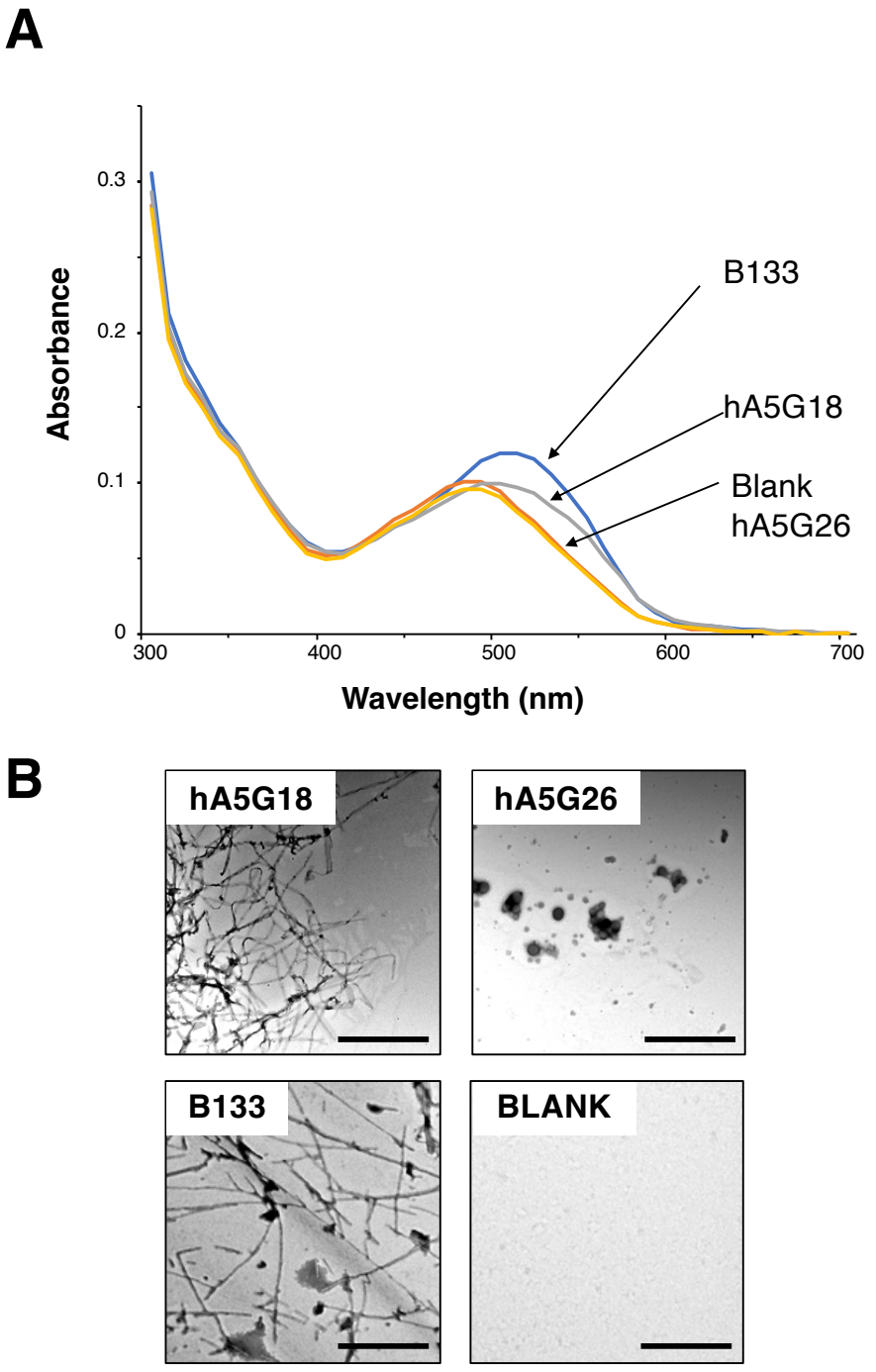

Figure 2. Congo red staining and electron micrographic analysis of peptides. (**A**) Absorption spectra of peptides with Congo Red were recorded from 300 to 700 nm. (**B**) Electron micrograph of amyloid-like fibrils formed from peptides. Peptide solution (1 mM) was diluted 1:0 to 1:4 with water and smear solution on a grid mesh with carbon-coated Formvar film. Then the specimen was negatively stained with a 2% aqueous solution of uranyl acetate and observed using an electron microscope. Bar = 500 nm.

2.2. Cell attachment activity and amyloid-like fibril formation of truncated hA5G18 peptides

Recently, Katagiri et al. reported that B133 exhibits cell attachment activity by forming amyloid-like fibrils [36, 49]. They performed a detailed analysis using the truncated peptide of B133. The results revealed that the N-terminal Asp contributes to the amyloid-like fibril formation, and the C-terminal Glu plays an essential role in integrin α2β1 binding [49]. Here, I focused on hA5G18 and examined active core sequences for the cell attachment activity and amyloid-like fibril formation using a set of truncated hA5G18 peptides.

First, the N-terminal truncated hA5G18 peptides have been synthesized and examined the cell attachment activity and amyloid-like fibril formation (**Table 1**).

Cell attachment activity of the N-terminal truncated hA5G18 peptides were examined in peptide-coated plate assay. AG73 was used as a positive control [9]. hA5G18A and hA5G18B promoted cell attachment in a dose-dependent manner similar to that of hA5G18 and AG73, but hA5G18C did not (**Figure 3A**).

When Congo red solution was incubated with the truncated peptides, the Congo red absorption peak at 490 nm was significantly shifted at 540 nm by hA5G18 similar to that by B133 (**Figure 3B**). In contrast, the N-terminal three amino acid deleted peptide hA5G18C did not influence the absorption spectrum. These results suggest that hA5G18A and hA5G18B are amyloidogenic but hA5G18C is not.

In the TEM analysis, hA5G18A and hA5G18B showed fibrils similar to that of B133, but hA5G18C did not show fibrils (**Figure 3C**). These results suggest that the third amino acid residue, phenylalanine, from the N-terminus, plays an essential role in the amyloid formation and cell attachment activity. These results also suggest that hA5G18B has both amyloid-like fibril formation and cell attachment activity similar to those of hA5G18.

Table 1. Biological activities of hA5G18 and N-terminal truncated hA5G18 peptides

Peptide	Sequence	Congo Red Staining [a]	Cell Attachment [b]	Cell Spreading [c]
hA5G18	DDFVFYVGGYPS	+	+	+
hA5G18A	DFVFYVGGYPS	+	+	+
hA5G18B	FVFYVGGYPS	+	+	+
hA5G18C	VFYVGGYPS	-	-	-

[a] Peptides were incubated with a Congo red solution, and the absorption spectra measuring from 300 to 700 nm were evaluated on the following subjective scale: + showed Congo red activity; and - no shift in the absorption peak. [b] Cell attachment activity was scored on the following subjective scale: + showed cell attachment activity, and - no activity. [c] Cell spreading activity was scored on the following subjective scale: + showed cell spreading activity; and - no activity.

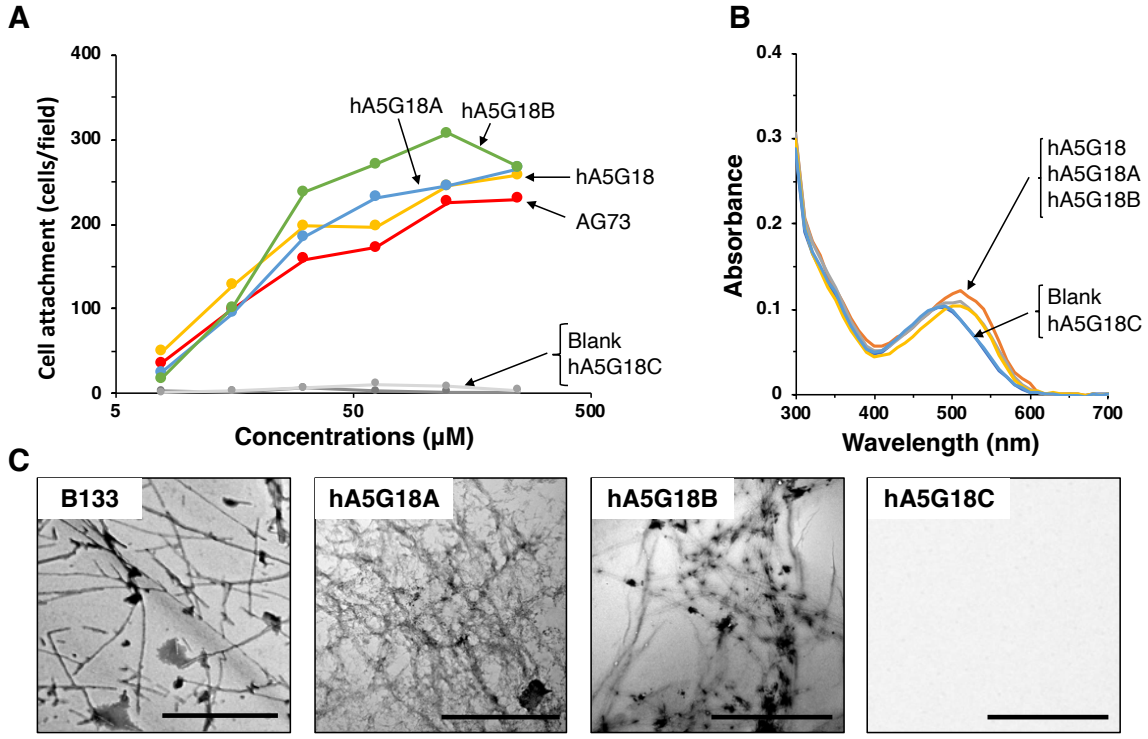

Figure 3. Amyloid-like fibril formation and cell attachment activity of the N-terminal truncated hA5G18 peptides. (**A**) Cell attachment of the N-terminal truncated hA5G18 peptides in a peptide-coated plate assay. Peptide-coated plates were prepared as described in the Materials and Method section, and HDFs (2×10^4 cells/well) were added and incubated for 1 hr. (**B**) Peptides were stained with Congo red, and absorption spectra were recorded from 300 to 700 nm. (**C**) Electron micrograph of peptides. Bars = 500 nm.

2.3. Cell attachment activity and amyloid-like fibril formation of C-terminal truncated hA5G18B peptides

Next, I focused on the hA5G18B peptide and C-terminal truncated hA5G18B peptides (hA5G18BTC1-6) were synthesized and their amyloid-like fibril formation and cell attachment activity were examined (**Table 2**).

When the C-terminal truncated hA5G18B peptides were examined in a cell attachment assay, none of the truncated peptides showed activity (**Figure 4A**). These results suggest that hA5G18B (FVFYVGGYPS) is the minimum active sequence for the cell attachment.

In Congo red staining assay, the C-terminal fifth amino acid deleted peptide hA5G18BTC5 still showed Congo red staining. When the C-terminal sixth amino acid valine was deleted, hA5G18BTC6 was eliminated the Congo red staining activity (**Figure 4B**). These results suggest that the FVFYV sequence is critical for the amyloid-like fibril formation of hA5G18B.

In TEM analysis, the hA5G18BTC1- hA5G18BTC5 peptides showed fibrils (**Figure 4C**). When the C-terminal sixth amino acid valine was deleted, hA5G18BTC6 did not show fibrils.

These results suggest that hA5G18BTC5 (FVFYV) is a minimum active sequence for amyloid-like fibril formation.

Table 2. Biological activities of truncated hA5G18 peptides

Peptide	Sequence	Congo Red Staining [a]	Cell Attachment [b]	Cell Spreading [c]
hA5G18BTC1	FVFYVGGYP	+	-	-
hA5G18BTC2	FVFYVGGY	+	-	-
hA5G18BTC3	FVFYVGG	+	-	-
hA5G18BTC4	FVFYVG	+	-	-
hA5G18BTC5	FVFYV	+	-	-
hA5G18BTC6	FVFY	-	-	-

[a] Peptides were incubated with a Congo red solution, and the absorption spectra measuring from 300 to 700 nm were evaluated on the following subjective scale: + showed Congo red activity; and - no shift in the absorption peak. [b] Cell attachment activity was scored on the following subjective scale: + showed cell attachment activity, and - no activity. [c] Cell spreading activity was scored on the following subjective scale: + showed cell spreading activity; and - no activity.

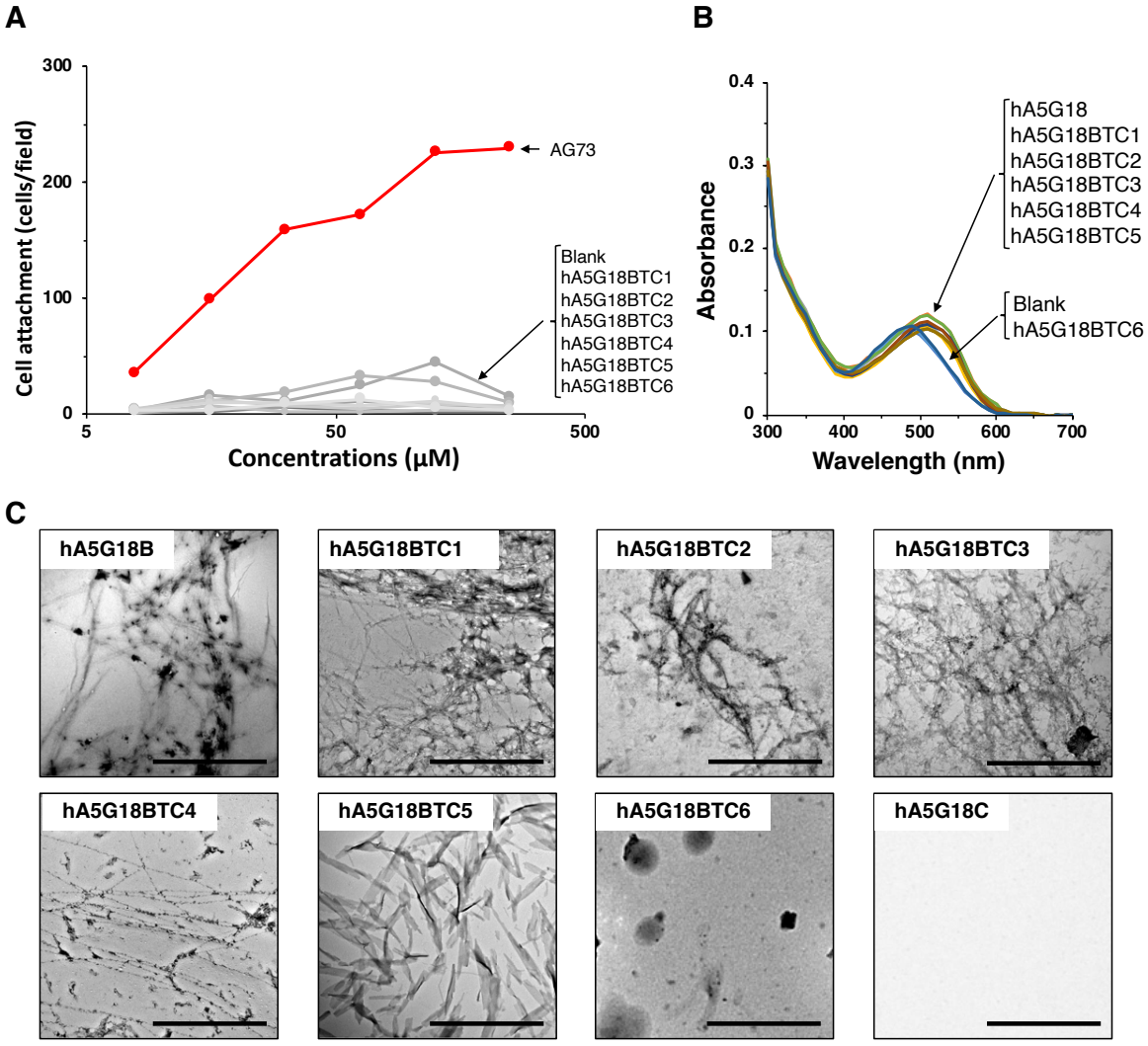

Figure 4. Amyloid-like fibril formation and cell attachment activity of the C-terminal truncated hA5G18B peptides. (**A**) Cell attachment of the C-terminal truncated hA5G18B peptides in a peptide-coated plate assay. Peptide-coated plates were prepared as described in the Materials and Method section, and HDFs (2×10^4 cells/well) were added and incubated for 1 hr. (**B**) Peptides were stained with Congo red, and absorption spectra were recorded from 300 to 700 nm. (**C**) Electron micrograph of peptides. Bars = 500 nm.

2.4. Cell attachment activity of hA5G18B conjugated Sepharose bead

I prepared the hA5G18B-conjugated Sepharose bead and tested cell attachment activity to evaluate the amyloid-like fibril formation requirement for the activity. AG73-conjugated Sepharose bead was used as a positive control. AG73-conjugated Sepharose bead showed cell attachment, but hA5G18B-conjugated Sepharose bead did not (**Figure 5**). These results suggest that the cell attachment activity of hA5G18B requires amyloid-like fibril formation.

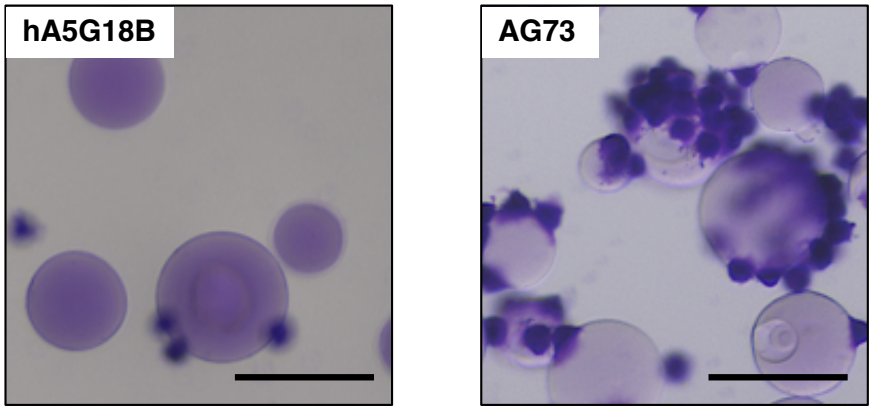

Figure 5. Cell attachment of peptide-Sepharose beads. HDFs were allowed to attach to peptide-Sepharose beads for 1 hr and then stained with 0.2% crystal violet in 20% methanol. Bar = 100 μm.

2.5. Alanine substituted analysis of hA5G18B

In molecular biology, alanine scanning is a technique that uses site-directed mutagenesis to determine the contribution of a specific residue to the stability or function of a given protein [50]. This technique can also be used to determine whether the side chain of any particular residue plays a significant role in bioactivity. The alanine scanning method takes advantage of the fact that most canonical amino acids can be exchanged with alanine by point mutations. At the same time, the secondary structure of the mutated protein is still stable. Because many side chains are analyzed simultaneously, the need for protein purification and biophysical analysis is circumvented [51].

Ten alanine-substituted hA5G18B peptides were synthesized to evaluate critical amino acids for the amyloid-like fibril formation and cell attachment activity (**Table 3**).

In Congo red staining assay, when the Val5, Gly6, Pro9, and Ser10 residues of hA5G18B

were substituted with alanine, the absorption peak at 490 nm was significantly shifted at 540 nm, similar to that by hA5G18B (**Figure 6**). The Congo red absorption peak was also weakly shifted by hA5G18BA7 (G) and hA5G18BA8 (Y). In contrast, hA5G18BA1 (F), hA5G18BA2 (V), hA5G18BA3 (F), and hA5G18BA4 (Y) did not influence on the absorption spectrum of Congo red. These results suggest that the Phe1, Val2, Phe3, and Tyr4 residues are critical residues for the amyloid-like fibril formation of hA5G18B, and the Gly7 and Tyr8 residues partially contribute to the amyloid-like fibril formation of hA5G18B.

Table 3. Biological activities of hA5G18B and its alanine-substituted derivatives

Peptide	Sequence [a]	Congo Red Staining [b]	Amyloid-like Fibril Formation [c]	Cell Attachment [d]	Cell Spreading [e]
hA5G18B	FVFYVGGYPS	+	+	+	+
hA5G18BA1(F)	**A**VFYVGGYPS	-	-	-	-
hA5G18BA2(V)	F**A**FYVGGYPS	-	-	-	-
hA5G18BA3(F)	FV**A**YVGGYPS	-	-	-	-
hA5G18BA4(Y)	FVF**A**VGGYPS	-	-	-	-
hA5G18BA5(V)	FVFY**A**GGYPS	+	+	+	+
hA5G18BA6(G)	FVFYV**A**GYPS	+	+	+	+
hA5G18BA7(G)	FVFYVG**A**YPS	+	+	+	+
hA5G18BA8(Y)	FVFYVGG**A**PS	+	+	+	+
hA5G18BA9(P)	FVFYVGGY**A**S	+	+	+	-
hA5G18BA10(S)	FVFYVGGYP**A**	+	+	+	+

a Substituted alanine is shown in bold. b Peptides were incubated with a Congo red solution. The absorption spectra measuring from 300 to 700 nm were evaluated on the following subjective scale: + showed Congo red activity, and - no shift in the absorption peak. c Peptides were examined by TEM and evaluated on the following subjective scale: + showed amyloid-like fibrils, and - no fibrils. d Cell attachment activities were scored on the following subjective scale: + showed cell attachment activity, and - no activity. e Cell spreading activity was scored on the following subjective scale: + showed cell spreading activity; and - no activity.

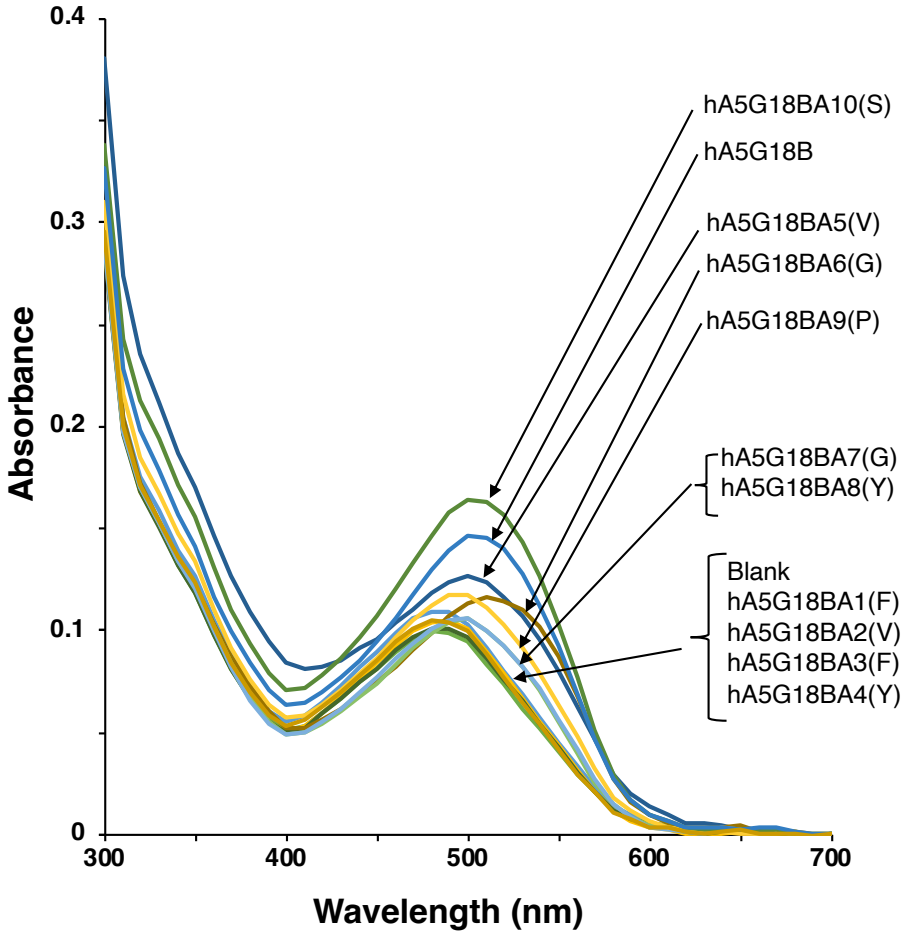

Figure 6. Amyloidogenicity of the Ala-substituted hA5G18B peptides. Absorption spectra of peptides stained with Congo Red. Peptide solution (100 μL, 1 mM in H_2O) and Congo red solution (100 μL, 100 μM in PBS) were mixed with 800 μL of PBS and incubated for 24 hrs at room temperature. Absorption spectra were recorded from 300 to 700 nm.

Next, amyloid-like fibril formation of the alanine-substituted hA5G18B peptides was examined by a TEM (**Figure 7**). hA5G18BA5 (V), hA5G18BA6 (G), hA5G18BA7 (G), hA5G18BA8 (Y), hA5G18BA9 (P), and hA5G18BA10 (S) showed fibrils as well as that of hA5G18B. In contrast, hA5G18BA1 (F), hA5G18BA2 (V), hA5G18BA3 (F), and hA5G18BA4 (Y) did not show fibrils. These results suggest that the Phe1, Val2, Phe3, and Tyr4 residues are critical residues for the amyloid-like fibril formation of hA5G18B.

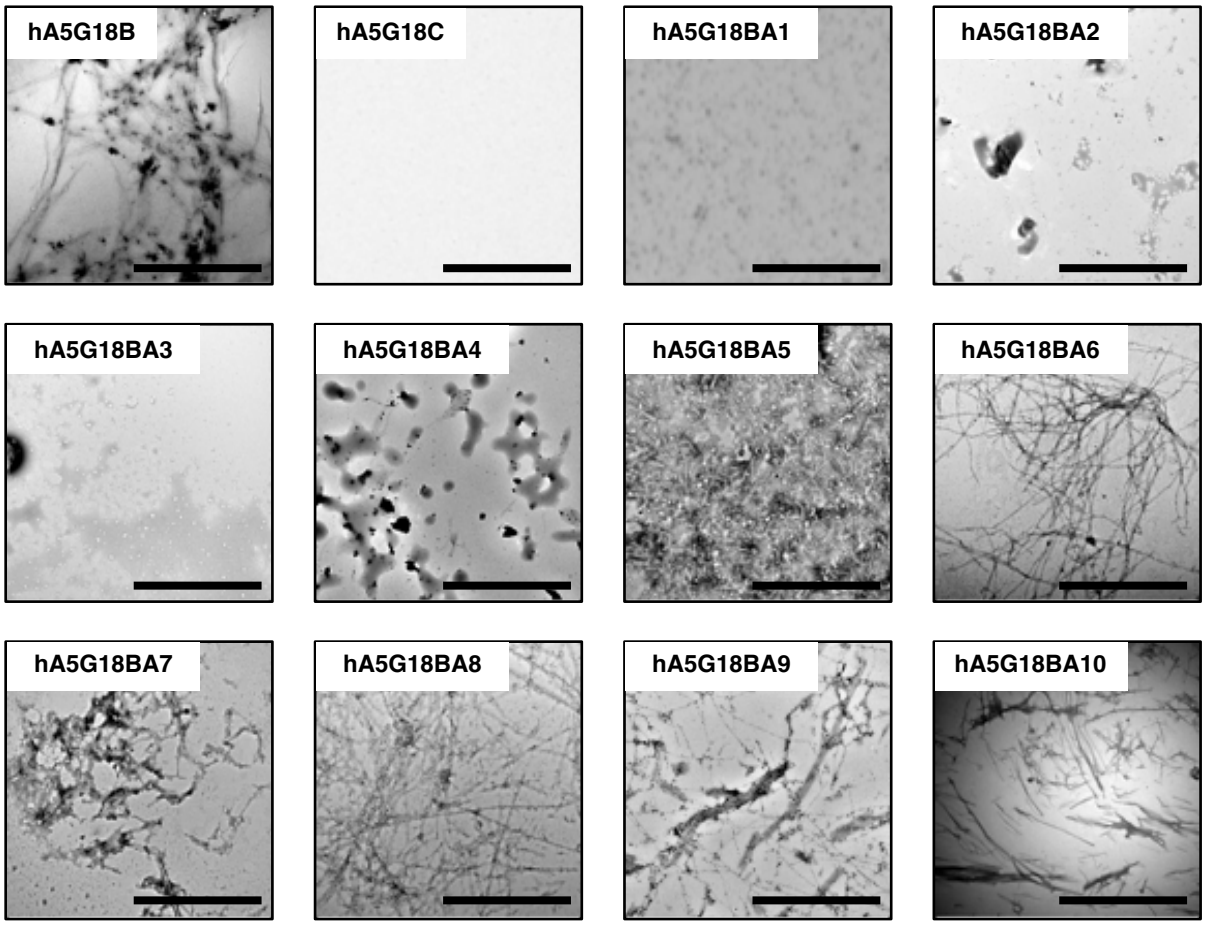

Figure 7. Electron micrographs of peptides. Bars = 500 nm.

Next, we evaluated the cell attachment activities of alanine-substituted hA5G18B peptides (**Table 3, Figure 8**). hA5G18BA5 (V), hA5G18BA6 (G), hA5G18BA7 (G), hA5G18BA8 (Y), hA5G18BA9 (P), and hA5G18BA10 (S) promoted cell attachment activity in a dose-dependent manner as well as that of hA5G18B. In contrast, the cell attachment activity was significantly decreased when the Phe1, Val2, Phe3, and Tyr4 residues were substituted with alanine. These results suggest that the Phe1, Val2, Phe3, and Tyr4 residues are critical for the cell attachment activity.

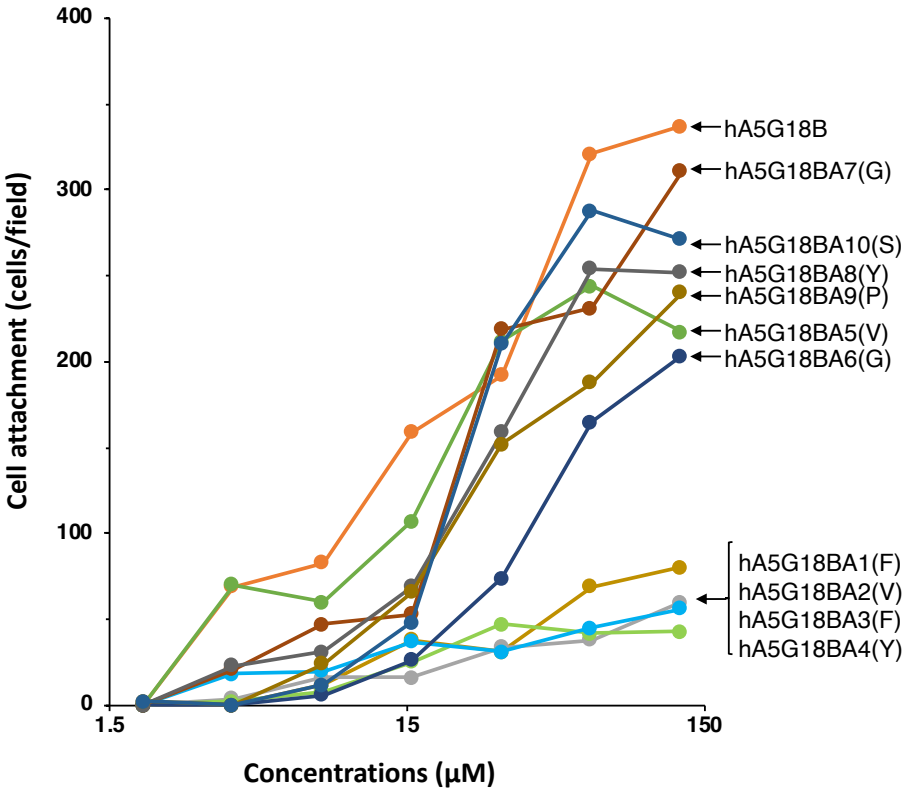

Figure 8. Cell attachment activity of the Ala-substituted hA5G18B peptides. Cell attachment activity of the Ala-substituted hA5G18B peptides. Peptide-coated plates were prepared as described in the Materials and Methods section, and HDFs (2×10^4 cells/well) were added and incubated for 1 hr. After being stained with 0.2% crystal violet in 20% methanol, the attached cells were counted. The data are expressed as the means of triplicate results.

2.6. Evaluation of cell morphology of alanine-substituted hA5G18B peptides

Cell morphology on the alanine-substituted hA5G18B peptides were examined (**Figure 9**). AG73 and hA5G18B were used as controls. hA5G18B promoted cell spreading, and AG73 did not. A5G18BA5 (V), hA5G18BA6 (G), hA5G18BA7 (G), hA5G18BA8 (Y), and hA5G18BA10 (S) promoted cell spreading similar to that of hA5G18B. Additionally, hA5G18BA9 (P) showed cell attachment and promoted a round shape cell morphology similar to that of AG73. In contrast, hA5G18BA1 (F), hA5G18BA2 (V), hA5G18BA3 (F), and hA5G18BA4 (V) did not show cell attachment. These results suggest that A5G18BA5 (V), hA5G18BA6 (G), hA5G18BA7 (G), hA5G18BA8 (Y), and hA5G18BA10 (S) promote integrin-mediated cell attachment and hA5G18BA9 (P) promotes syndecan-mediated cell attachment.

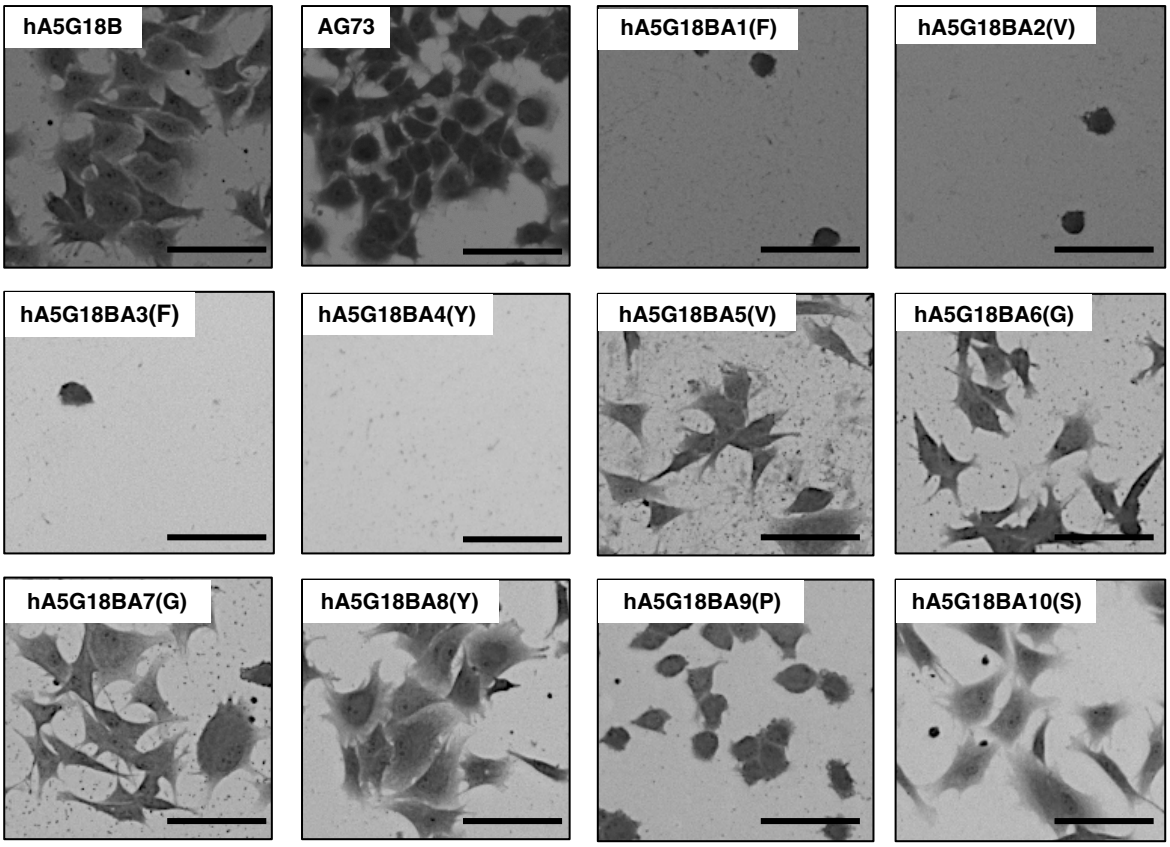

Figure 9. Morphological appearance of HDFs on peptide-coated plates. Peptides (2 nmol/well of hA5G18B and hA5G18BA1-10, 0.4 nmol/well of AG73) were coated on plates, and HDFs (2×10^4 cells/well) were added. After a 1 hr incubation, cells were stained with 0.2% crystal violet in 20% methanol. Bar = 100 μm.

2.7. Homologous sequences of FVFYV

Homologous sequences of FVFYV were analyzed. Previously, Katagiri et al. identified an FVFYV containing peptide A5G15 (HPDDFVFYVGGY) from the mouse laminin α5 chain G domain [66]. A5G15 promoted cell attachment and spreading in the peptide-coated plate assay but did not show cell attachment activity in the peptide-conjugated Sepharose beads assay. Additionally, cell attachment of the peptide was inhibited by EDTA. These results suggest that the A5G15 peptide forms amyloid-like fibrils and promotes an integrin-mediated cell attachment. The homology between mouse laminin α5 chain and human laminin α5 chain peptide sequence is about 79% [25,26]. A homologous peptide of the mouse laminin peptide A5G15 was designed using the human laminin sequence as hA5G178 (between hA5G17 and thA5G18) (**Figure 10**). I evaluated biological activity of hA5G178 and its active core sequence for amyloid fibril formation and cell attachment activity.

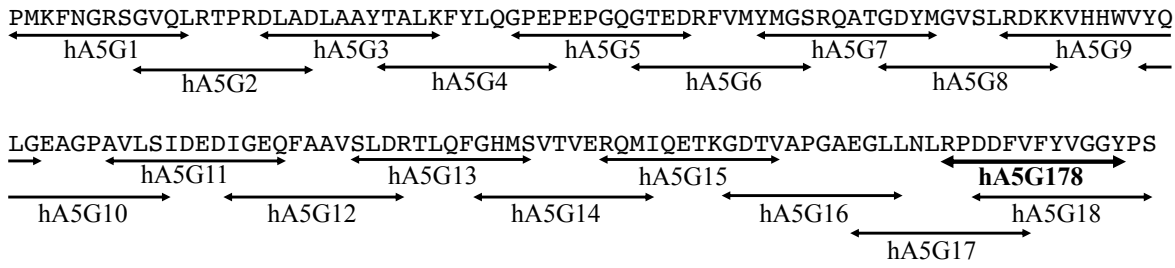

Figure 10. Sequences and peptides from the laminin α5 G domain. Arrows indicate the location of peptides. The peptide hA5G178 and the sequence are shown by bold.

2.8. Cell attachment activity and amyloid-like fibril formation of C-terminal truncated hA5G178 peptides

First, I synthesized the truncated peptides from the C-terminal based on hA5G178. Six peptides (hA5G178TC1-TC6) were synthesized by truncating one by one residue from the C-terminus of hA5G178 (**Table 6**). hA5G178 as the positive was used as a control for Congo red staining assay. The C-terminal truncated hA5G178 peptides were examined in the cell attachment assay and Congo red staining assay.

Table 6. Biological activities of hA5G178 and C-terminal truncated hA5G178 peptides

Peptide	Sequence	Congo Red Staining [a]	Cell Attachment [b]	Cell Spreading [c]
hA5G178	RPDDFVFYVGGY	+	++	+
hA5G178TC1	RPDDFVFYVGG	+	++	+
hA5G178TC2	RPDDFVFYVG	+	++	+
hA5G178TC3	RPDDFVFYV	+	++	+
hA5G178TC4	RPDDFVFY	+	+	+
hA5G178TC5	RPDDFVF	-	-	-
hA5G178TC6	RPDDFV	-	-	-

[a] Peptides were incubated with a Congo red solution, and the absorption spectra measuring from 300 to 700 nm was evaluated on the following subjective scale: + showed Congo red activity; and - no shift in the absorption peak. [b] Cell attachment activity was scored on the following subjective scale: ++ showed the same cell attachment activity as the hA5G178; + showed weak cell attachment activity; and - no activity. [c] Cell spreading activity was scored on the following subjective scale: + showed cell spreading activity; and - no activity.

From Congo red staining assay, the result suggests that when Congo red solution was incubated with the truncated peptides, the hA5G178TC1, hA5G178TC2, hA5G178TC3, and hA5G178TC4 peptides were observed to shift the maximum absorption wavelength to the longer wavelength side (**Figure 11A**), which is characteristic of amyloid-like fibril formation. But we can see that when C-terminal four amino acids were deleted, the absorbance intensity of the hA5G178TC4 peptide decreased significantly. When the C-terminal five amino acids were deleted, the absorbance curve of hA5G178TC5 was almost identical to that of the blank. This result indicated that C-terminus fifth amino acid Tyrosine plays an essential role in the

hA5G178 sequence in forming amyloid-like fibrils.

Further, we examined cell attachment activity of the C-terminal truncated hA5G178 peptides. The result suggests that hA5G178TC1, hA5G178TC2, and hA5G178TC3 promoted cell attachment in a dose-dependent manner similar to that of hA5G178 (**Figure 11B**) when the C-terminal four amino acids were deleted, the cell attachment activity of the hA5G178TC4 peptide decreased significantly. However, it still showed some activity. When the C-terminal five amino acids were deleted, the hA5G178TC5 peptide exhibited a slightly higher cell attachment activity strength than the blank. It can be concluded that hA5G178TC5 does not have cell attachment activity, and the C-terminus fifth amino acid Tyrosine plays an essential role in the hA5G178 sequence in cell attachment activity.

These results suggest that hA5G178TC4 is the minimal essential sequence in the C-terminal truncated hA5G178 peptides in forming amyloid-like fibrils and cell attachment activity.

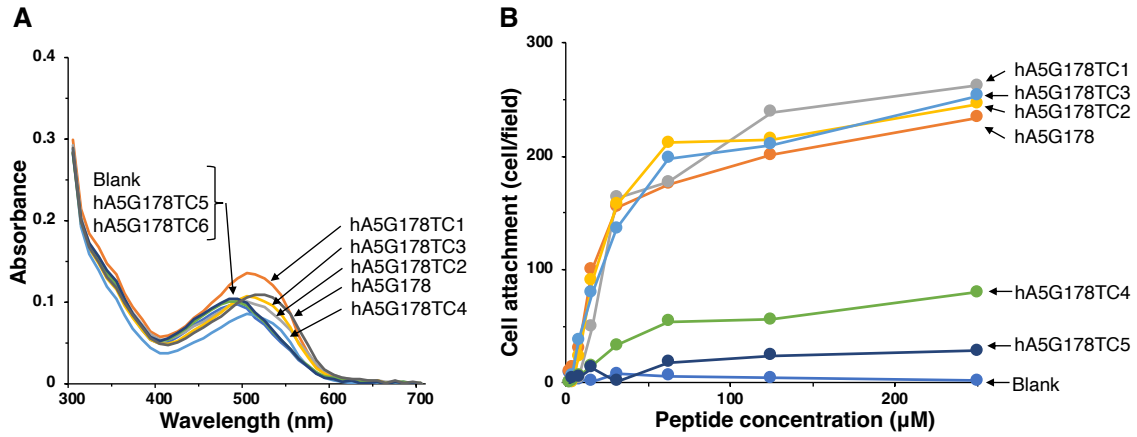

Figure 11. Amyloid-like fibril formation and cell attachment activity of the C-terminal truncated hA5G178 peptides. (**A**) Peptides were stained with Congo red, and absorption spectra were recorded from 300 to 700 nm. (**B**) Cell attachment of the C-terminal truncated hA5G178 peptides in a peptide-coated plate assay. Peptide-coated plates were prepared as described in the Materials and Method section, and HDFs (2×10^4 cells/well) were added and incubated for 1 hr.

2.9. Cell attachment activity and amyloid-like fibril formation of N-terminal truncated hA5G178TC4 peptides

Based on the conclusion of the previous section, I focused on the hA5G178TC4 peptide and synthesized N-terminal truncated peptides of hA5G178TC4. Three peptides (hA5G178TN1TC4, hA5G178TN2TC4, and hA5G178TN3TC4) were synthesized by truncating one by one residue from the N-terminus of hA5G178TC4 (**Table 7**). The N-terminal truncated hA5G178TC4 peptides were evaluated their amyloid-like fibril formation and cell attachment activity. hA5G178TN1TC4 showed Congo red staining but did not promote cell attachment activity (**Table 7**). hA5G178TN2TC4 and hA5G178TN3TC4 were not examined in a Congo red staining and cell attachment assays because of their insolubility in water.

Table 7. Biological activities of hA5G178TC4 and N-terminal truncated hA5G178TC4 peptides

Peptide	Sequence	Congo Red Staining [a]	Cell Attachment [b]	Cell Spreading [c]
hA5G178TC4	RPDDFVFY	+	+	+
hA5G178TN1TC4	PDDFVFY	+	-	-
hA5G178 TN2TC4	DDFVFY	N.D.	N.D.	N.D.
hA5G178 TN3TC4	DFVFY	N.D.	N.D.	N.D.

N.D.: not determined

The hA5G178TN1TC4 peptide showed a wavelength shift and the maximum absorption wavelength to the longer wavelength side in the Congo red assay similar to that of hA5G178TC4 (**Figure 12A**). When the first amino acid arginine at the N-terminus was deleted, the absorbance intensity increased significantly. hA5G178TN1TN4 was suggested to form amyloid-like fibrils. hA5G178TN2TC4 and hA5G178TN3TC4 were insoluble in water. hA5G178TN1TC4 (PDDFVFY) is suggested a core sequence for the amyloid-like fibril formation of hA5G178.

Cell attachment assay was examined for hA5G178, hA5G178TC4, and hA5G178TN1TC4 (**Figure 12B**). hA5G178TC4 showed cell attachment activity but hA5G178TN1TC4 did not. hA5G178TC4 (RPDDFVFY) is suggested to be a minimal essential sequence of hA5G178 for the cell attachment activity.

From the previous results of Chapter 1, I can figure out that FVFY itself cannot form amyloid-like fibrils. However, whether adding Pro-Asp-Asp to the N-terminus or adding Valine to the C-terminus can form amyloid-like fibrils. The PDDFVFYV sequence may have a better effect of forming amyloid-like fibrils.

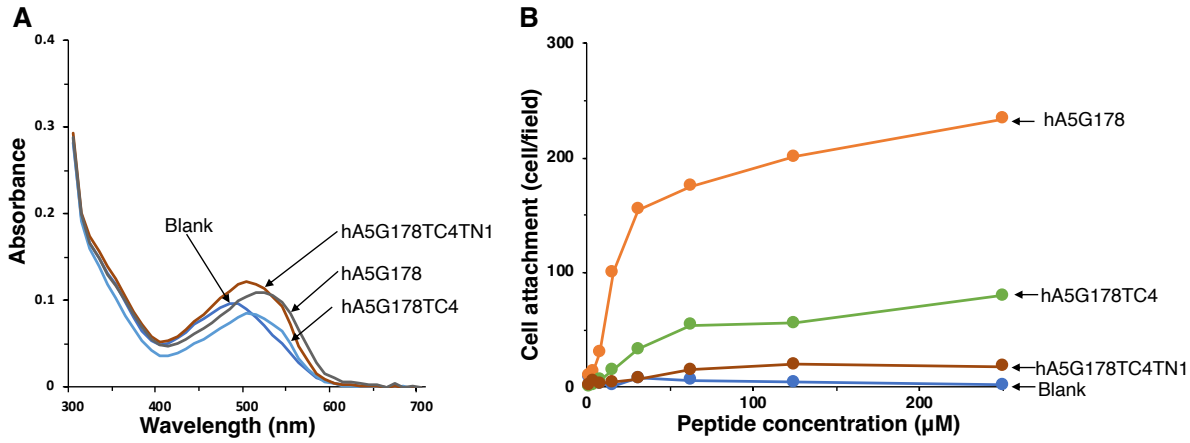

Figure 12. Amyloid-like fibril formation and cell attachment activity of the N-terminal truncated hA5G178TC4 peptides. (**A**) Peptides were stained with Congo red, and absorption spectra were recorded from 300 to 700 nm. (**B**) Cell attachment of the N-terminal truncated hA5G178TC4 peptides in a peptide-coated plate assay. Peptide-coated plates were prepared as described in the Materials and Method section, and HDFs (2×10^4 cells/well) were added and incubated for 1 hr.

3.Conclusion

In chapter 1, I focus on the hA5G18 peptide and, using a Congo red staining assay and an electron microscopic analysis, describe how this peptide forms amyloid-like fibrils by a Congo red staining assay and an electron microscopic analysis. hA5G18 was active in the plate assay but inactive in the Sepharose bead assay. These results suggest that amyloid-like fibril formation is required for the cell attachment activity of hA5G18. The deletion analysis showed that FVFYV is an essential sequence for amyloid-like fibril formation but is not active in cell attachment. The FVFYV sequence can be used as the core sequence for forming amyloid-like fibrils. I found a peptide sequence containing FVFYV from mouse laminin α5 chain G domain named A5G15, and an almost identical sequence was found at human laminin α5 chain G

domain, which we named hA5G178. The truncated analysis revealed that FVFY contribute to form amyloid-like fibril formation and a cell attachment activity core sequence is hA5G178TN4 (RPDDFVFY). FVFYV is useful as a core sequence for amyloid-like fibrils

Chapter 2: Application of FVFYV for functional amyloid-like fibrils as a biomaterial

1. Introduction

Tissue engineering has been widely used therapeutically in the past decade [52]. Many polymers have been developed as biomaterials that can specifically bind to cells and provide mechanical support to form tissue spaces. ECM is a highly complex scaffold composed of variety of biologically active molecules such as collagen, laminin, perlecan, and nidogen, and active peptide conjugated polymers have been developed as a functional biomaterial [53-56]. Arg-Gly-Asp (RGD) sequence, as the first peptide discovered as an integrin ligand, has been widely used in molecular biology targeted drug delivery and ECM behavior modeling [57, 58].

In this study, I designed functional amyloid-like fibrils using the FVFYV peptide as a core sequence for amyloid-like fibrils for a cell scaffold material.

2. Results and Discussion

2.1. Conjugation of an RGD sequence to FVFYV

FVFYV was used as an amyloid-like fibril template and modified with a cell adhesive peptide (Table 8). An integrin binding sequence RGD was conjugated to FVFYV with Gly-Gly (GG) as a spacer. Arg-Gly-Glu (RGE), a negative control sequence of RGD, was also conjugated to FVFYV as a control.

Table 8. Biologically active peptide conjugated FVFYV peptides

Sequence	Congo Red Staining [a]	Cell Attachment [b]	Cell Spreading [c]
FVFYVGGRGD	+	+	+
FVFYVGGRGE	+	+	+

[a] Peptides were incubated with a Congo red solution, and the absorption spectra measuring from 300 to 700 nm were evaluated on the following subjective scale: + showed Congo red activity; and - no shift in the absorption peak. [b] Cell attachment activities were scored on the following subjective scale: + showed cell attachment activity, and - no activity. [c] Cell spreading activity was scored on the following subjective scale: + showed cell spreading activity; and - no activity.

2.2. Biological activity of RGD conjugated FVFYV peptide

When FVFYVGGRGD and FVFYVGGRGE were incubated with Congo red solution, the Congo red absorption peak at 490 nm was significantly shifted at 540 nm (**Figure 13A**). These

results suggest that FVFYVGGRGD and FVFYVGGRGE are amyloidogenic and form amyloid-like fibrils.

FVFYVGGRGD showed cell attachment activity in a dose-dependent manner in a peptide-coated plate assay (**Figure 13B**). However, FVFYVGGRGE also promoted cell attachment similarly. These results suggest that the cell attachment activity of FVFYVGGRGD in the peptide coated-plate assay is not due to the integrin binding sequence RGD, and the Arg residue in amyloid-like fibrils may cause the activity.

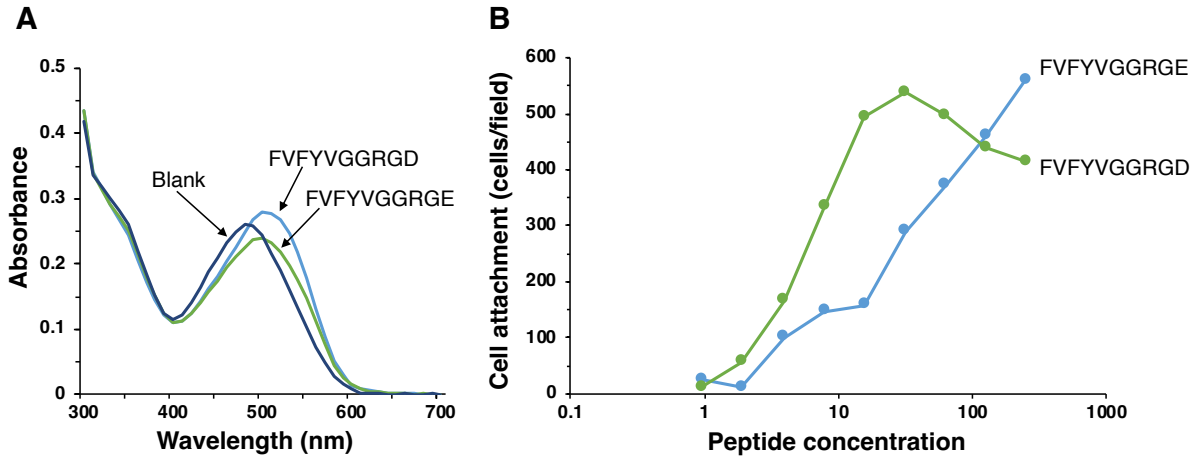

Figure 13. Amyloidogenicity and cell attachment activity of modified FVFYV peptides. (A) Absorption spectra of peptides stained with Congo Red. Peptide solution (100 μL, 1 mM in H2O) and Congo red solution (100 μL, 100 μM in PBS) were mixed with 800 μL of PBS and incubated for 24 hrs at room temperature. Absorption spectra were recorded from 300 to 700 nm. (B) HDFs attachment to peptide-coated plates. Peptide-coated plates were prepared as described in the Materials and Method section. HDFs (2×10^4 cells/well) were added to the wells and incubated for 1 hr. After being stained with 0.2% crystal violet in 20% methanol, the attached cells were counted. The data are expressed as the means of triplicate results. Triplicate experiments gave similar results.

2.3. Conjugation of basic amino acids to FVFYV

Various amyloidogenic peptides have been identified and many of the peptides promote cell attachment [35]. Additionally, most of the cell adhesive amyloidogenic peptides contain basic amino acids. To evaluate the effect of basic amino acids on the cell attachment activity of amyloid-like fibrils, I conjugated basic amino acids, Arg, Lys, and His, to the C-terminus of FVFYV with Gly-Gly as a spacer (**Table 9**). Additionally, I conjugated an Arg residue to the N-terminus of FVFYV with Gly-Gly as a spacer. When the Congo red solution was incubated with the peptides, the absorption peak at 490 nm was significantly shifted at 540 nm by all the peptides. These results suggest that the basic amino acid-conjugated FVFYV peptides form

amyloid-like fibrils (**Figure 14**).

Table 9. Biological activities of modified FVFYV peptides

Sequence	Congo Red Staining [a]	Cell Attachment [b]	Cell Spreading [c]
FVFYVGGR	+	+	+
FVFYVGGK	+	+	+
FVFYVGGH	+	-	-
RGGFVFYV	+	+	+

[a] Peptides were incubated with a Congo red solution, and the absorption spectra measuring from 300 to 700 nm were evaluated on the following subjective scale: + showed Congo red activity; and - no shift in the absorption peak. [b] Cell attachment activities were scored on the following subjective scale: + showed cell attachment activity, and - no activity. [c] Cell spreading activity was scored on the following subjective scale: + showed cell spreading activity; and - no activity.

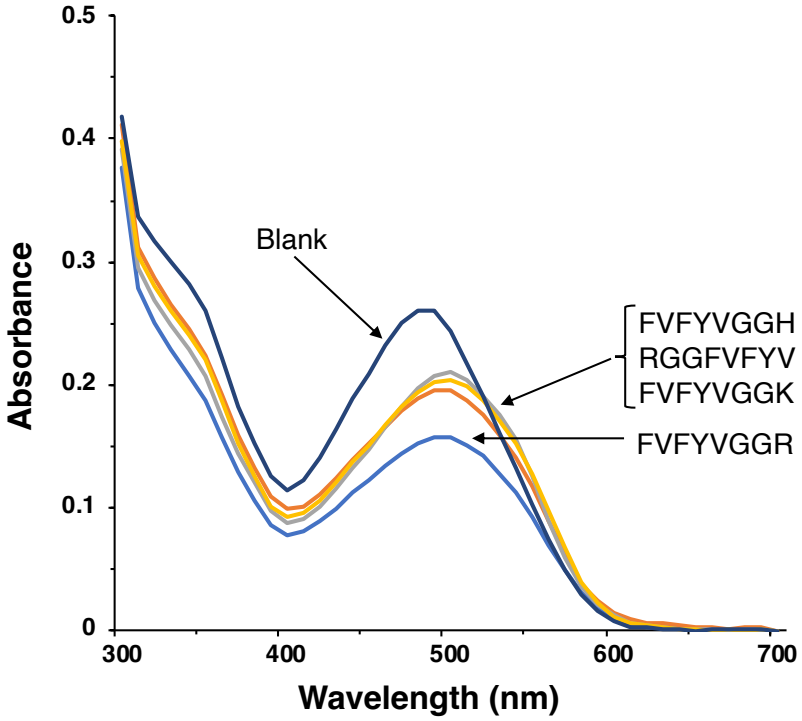

Figure 14. Amyloidogenicity of modified FVFYV peptides. Absorption spectra of peptides stained with Congo Red. Peptide solution (100 µL, 1 mM in H_2O) and Congo red solution (100 µL, 100 µM in PBS) were mixed with 800 µL of PBS and incubated for 24 hrs at room temperature. Absorption spectra were recorded from 300 to 700 nm.

Cell attachment activity of the basic amino acid conjugated FVFYV peptides were examined (**Figure 15**). FVFYVGGR and FVFYVGGK promoted cell attachment in a dose-

dependent manner. Additionally, RGGFVFYV also promoted cell attachment in a dose-dependent manner. In contrast, FVFYVGGH did not promote cell attachment, similarly to that of FVFYV. These results suggest that Arg and Lys residues contribute to the cell attachment activity in amyloid-like fibrils.

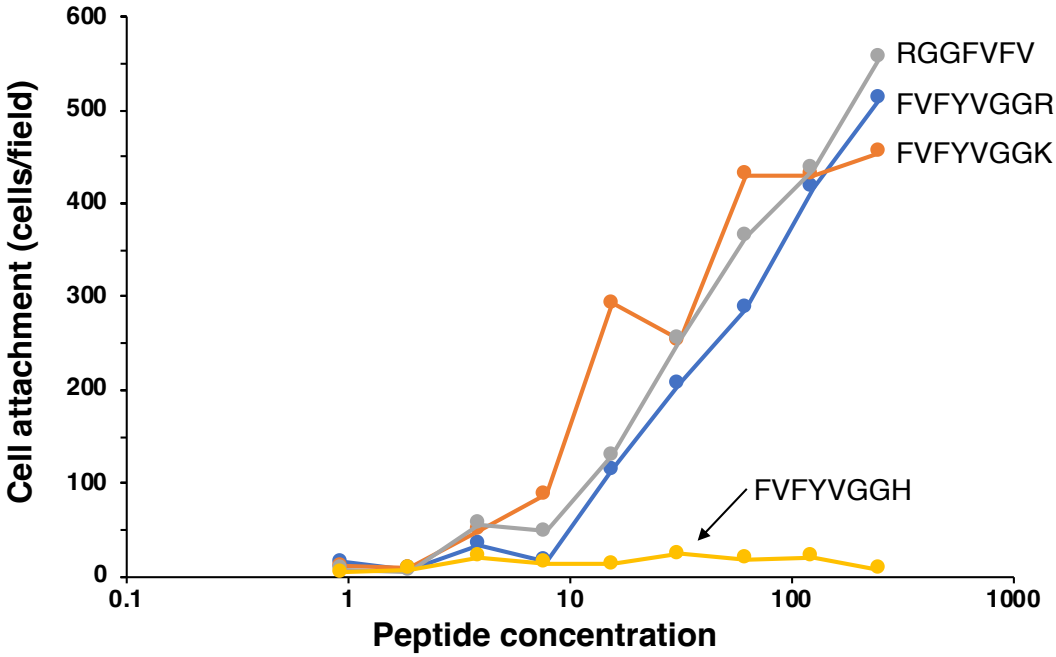

Figure 15. Cell attachment activity of modified FVFYV peptides. HDFs attachment to peptide-coated plates. Peptide-coated plates were prepared as described in the Materials and Method section. HDFs (2×10^4 cells/well) were added to the wells and incubated for 1 hr. After being stained with 0.2% crystal violet in 20% methanol, the attached cells were counted. The data are expressed as the means of triplicate results. Triplicate experiments gave similar results.

2.4. Sepharose beads assay of modified FVFYV peptides

Next, FVFYVGGRGD, FVFYVGGRGE, FVFYVGGR, FVFYVGGK, FVFYVGGH, and RGGFVFYV were conjugated to Sepharose beads and examined the cell attachment activity. AG73 bead was used as a positive control. AG73 bead showed cell attachment activity as shown previously [10]. The FVFYVGGRGD bead promoted cell attachment, but the other peptide beads did not show the activity (**Figure 16**). These results suggest that FVFYVGGRGD is active in the disaggregated condition, but the other peptides are required for amyloid-like fibril formation for the cell attachment activity.

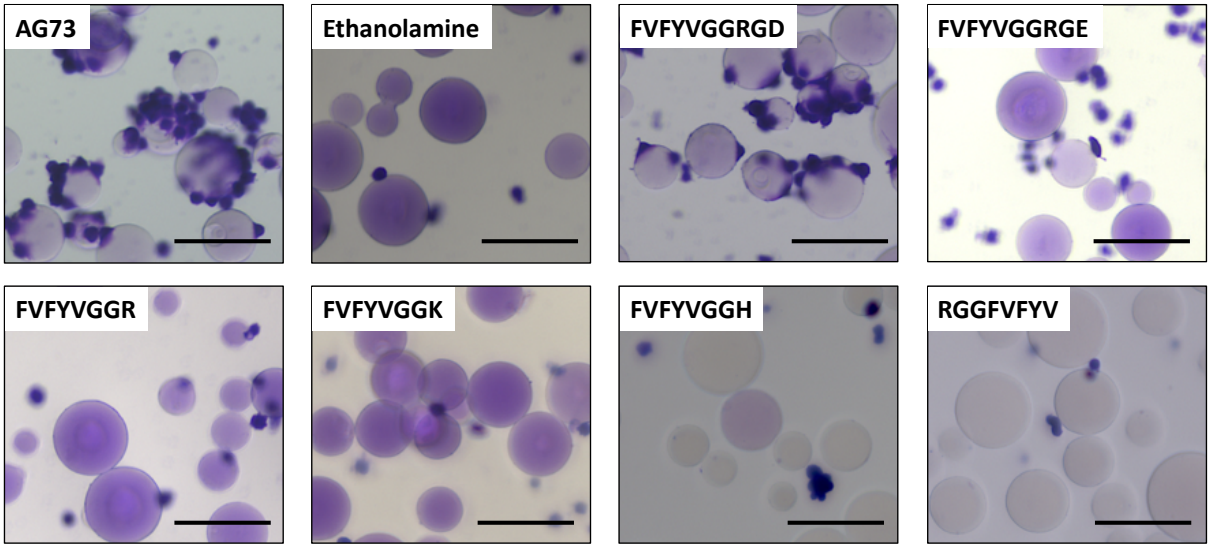

Figure 16. Amyloidogenicity of modified FVFYV peptides. Cell attachment to the peptide-Sepharose beads. HDFs were allowed to attach to the peptide Sepharose beads for 1 hr and then were stained with 0.2% crystal violet in 20% methanol. Bar = 100 nm.

2.5. Effect of EDTA and heparin on cell attachment to modified FVFYV peptides

The integrin family and syndecans, a membrane associated HSPG, are known to be the primary receptor on the cell surface. They are both located on the plasma membrane. The syndecan mediated cell adhesion occurs by ligands binding to extracellular heparan sulfate chains. Heparin inhibits the syndecan mediated cell adhesion by directly binding to the ligands. Integrins are a transmembrane heterodimer composed of two non-covalently bound transmembrane subunits, integrin α and β subunits. The binding of integrins to matrix proteins requires the participation of divalent cations, such as Ca^{2+} and Mg^{2+}. EDTA, a chelating agent, inhibits integrin mediated cell adhesion.

We examined the effect of EDTA and heparin on the cell attachment to FVFYVGGRGD, FVFYVGGRGE, FVFYVGGR, and FVFYVGGK to determine the cellular receptors in a peptide-coated plate assay (**Figure 17**). Additionally, we also examined poly-arginine (poly-R). EF1 was used as the EDTA inhibition control to interact with integrin α2β1 and promote divalent cation-dependent cell adhesion [63]. AG73 was used as a control to interact with syndecans and promote heparin-dependent cell attachment [19]. Cell attachment to EF1 was inhibited by EDTA but not by heparin, and that to AG73 was inhibited by heparin but not by EDTA, as shown previously [63]. The cell attachment to FVFYVGGRGD, FVFYVGGRGE, FVFYVGGR, FVFYVGGK, and poly-R was inhibited by both EDTA and heparin. These results suggest that the cell attachment of FVFYVGGR, FVFYVGGK, FVFYVGGRGD, FVFYVGGRGE, and poly-R is mediated by integrins and HSPGs.

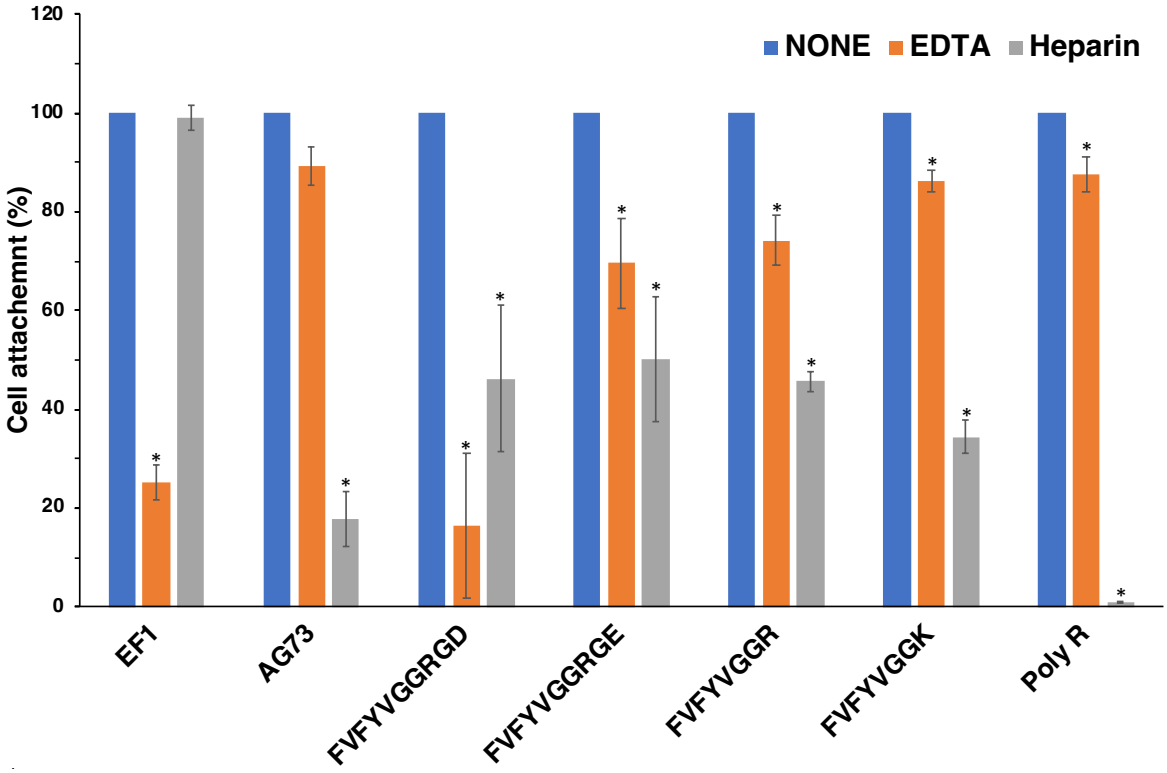

Figure 17. Effect of EDTA and heparin on cell attachment to the peptides. 96-well plate was coated with peptides (2 nmol/well of EF1, 0.4 nmol/well of AG73, 5 nmol/well of FVFYVGGRGD and FVFYVGGRGE, 10 nmol/well of FVFYVGGR and FVFYVGGK, 1 ng/well of poly R). HDFs were mixed with either 5 mM EDTA or 10 μg/mL heparin and then added to the plates. After a 1 hr incubation, cells were stained with crystal violet, and the number of the attached cells was counted. Each value represents the mean of three separate determinations ± S.D. Triplicate experiments gave similar results. * $p < 0.05$.

2.6. Effect of anti-integrin antibodies on cell attachment and spreading to to modified FVFYV peptides

Next, I examined the effect of anti-integrin antibodies on the cell attachment to FVFYVGGR, FVFYVGGK, FVFYVGGRGD, FVFYVGGRGE, and poly-R (**Figure 18**). EF-1 was used as a control. We used antibodies against integrin αvβ3, α2β1, α3/α6, and β1 [59,65]. As shown previously, the cell attachment to EF-1 was inhibited by anti-integrin α2β1 and β1 antibodies. Additionally, the cell attachment to EF-1 was weakly inhibited by the anti-integrin α3/α6 antibody [63]. The cell attachment to FVFYVGGRGD, FVFYVGGRGE, FVFYVGGR, FVFYVGGK, and poly-R was significantly inhibited by the anti-integrin β1 antibody. In contrast, the other anti-integrin antibodies did not influence cell attachment (**Figure 18**). These results suggest that integrin β1 is involved in the cell attachment to FVFYVGGRGD, FVFYVGGRGE, FVFYVGGR, FVFYVGGK, and poly-R.

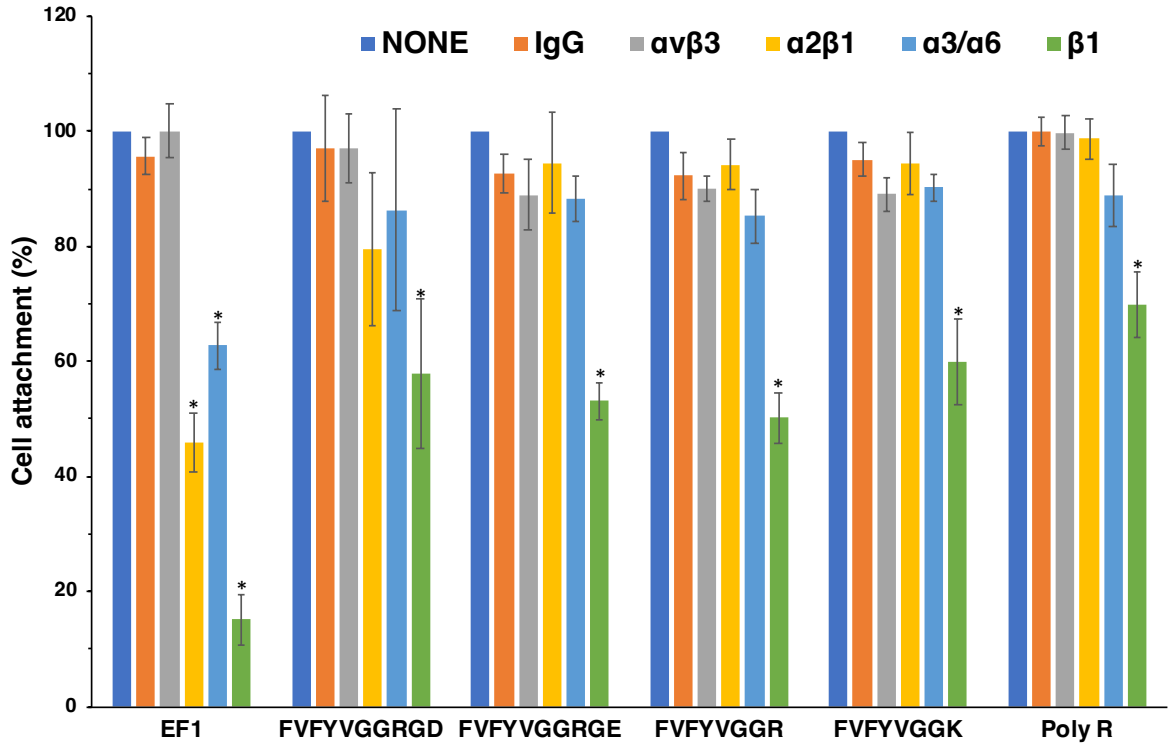

Figure 18. Effect of anti-integrin antibodies on cell attachment to peptides. HDFs were preincubated with 10 μg/mL of the integrin antibodies at room temperature for 15 min and added to the peptide-coated plates (2 nmol/well of EF1, 5 nmol/well of FVFYVGGRGD and FVFYVGGRGE, 10 nmol/well of FVFYVGGR and FVFYVGGK, 1 ng/well of poly R). After a 1 h incubation, cells were stained with crystal violet, and the number of the attached cells was counted. Each value represents the mean of three separate determinations ± S.D. Triplicate experiments gave similar results. * $p < 0.05$.

Further, we examined the effect of an integrin antibody on cell morphology. EF-1, FVFYVGGRGD, FVFYVGGRGE, FVFYVGGR, FVFYVGGK, and poly-R was significantly inhibited by the anti-integrin β1 antibody (**Figure 19**). Additionally, the cell spreading on all peptides, including FVFYVGGRGD, was not inhibited by the anti-αvβ3 and anti-integrin α3/α6 antibodies (data not shown). These results suggest that FVFYVGGRGD, FVFYVGGRGE, FVFYVGGR, FVFYVGGK, and poly-R promote integrin β1-mediated cell spreading.

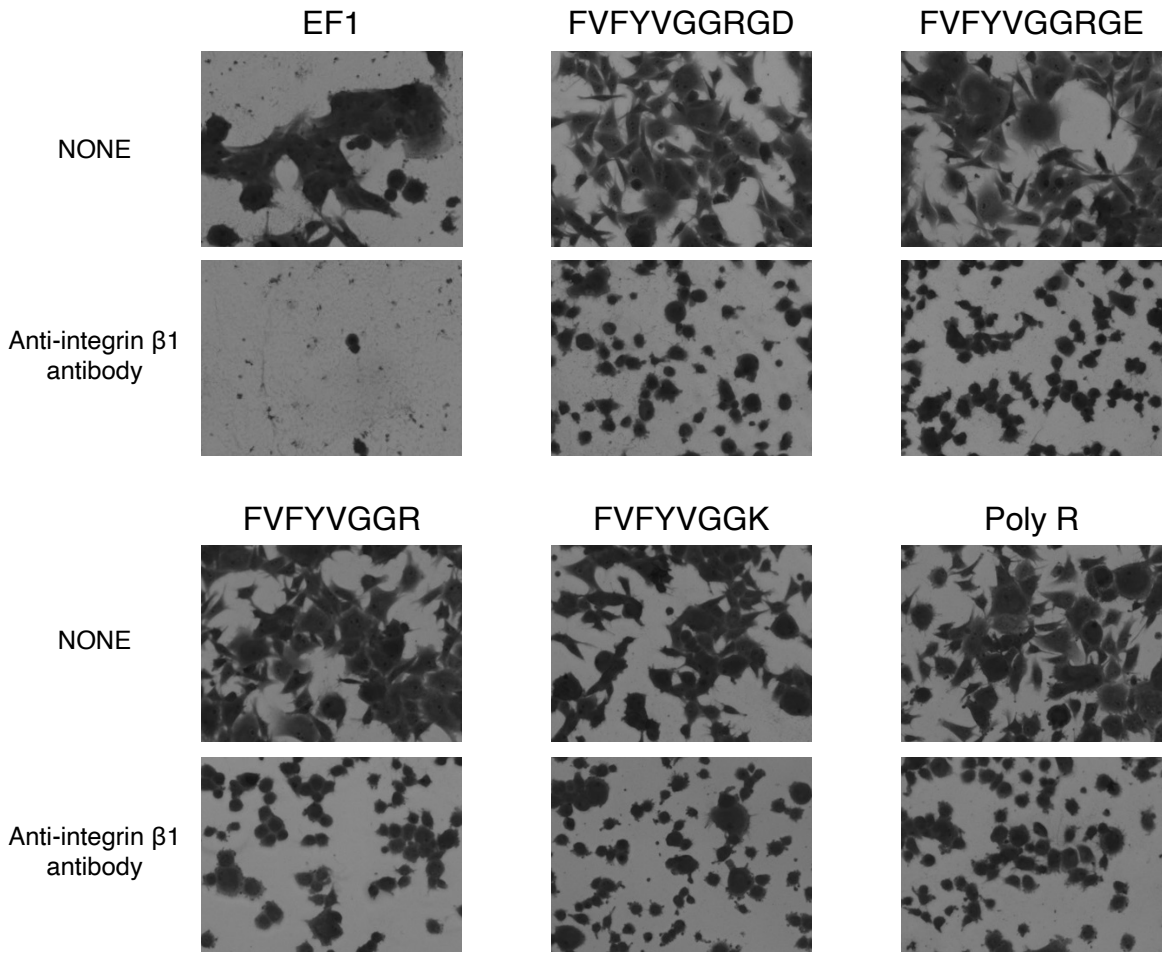

Figure 19. Effect of anti-integrin β1 antibody on cell adhesion to peptides. HDFs were preincubated with 10 μg/mL of integrin β1 antibody at room temperature for 15 min and added to the pep-tide-coated plates (2 nmol/well of EF1, 5 nmol/well of FVFYVGGRGD and FVFYVGGRGE, 10 nmol/well of FVFYVGGR and FVFYVGGK, 1 ng/well of poly R). After incubation for 1 hr, cells were stained with 0.2% crystal violet in 20% methanol.

3. Conclusion

In chapter 2, I designed a functional amyloid-like fibril using an integrin αvβ3 binding sequence RGD and FVFYV with GG as a spacer and analyzed their amyloidogenicity and cell attachment activity on the peptide-coated plate. The results suggest the RGD conjugated the FVFYV peptide FVFYVGGRGD and the negative control FVFYVGGRGE formed amyloid-like fibrils and similarly promoted cell attachment. The Arg residue is sought to contribute the activity. Previously it has been described that basic amino acids in amyloidogenic peptides are essential for cell attachment activity through HSPGs, such as syndecans [35, 36]. The basic amino acids (Arg, Lys, and His) were conjugated to the FVFYV peptide with GG as a spacer and examined their activity. The three peptides were stained with Congo red, suggesting that they form amyloid-like fibrils. FVFYVGGR and FVFYVGGK promoted cell attachment activity, but FVFYVGGH did not. These results suggest that His residue is weakly basic and does not contribute to the activity. Additionally, FVFYVGGR and FVFYVGGK promote integrin-mediated cell attachment. These results suggest that Arg and Lys residues promote cellular effects when incorporated in amyloid-like peptide fibrils. However, polymerized basic amino acids, such as poly-R, promoted integrin β1-mediated cell adhesion similar to FVFYVGGR and FVFYVGGK. The cell attachment of poly-R was completely inhibited by heparin and weakly inhibited by the EDTA and anti-integrin β1 antibody. However, the cell spreading of poly-R was completely inhibited by the anti-integrin β1 antibody. Since poly-R is highly basic and interacts strongly with HSPG, it may be difficult to find the effect of EDTA and the anti-integrin β1 antibody. Polymerized basic amino acids in polymers or fibrils have the potential to interact with heparin and integrin β1 [67]. Various amyloidogenic peptides have previously been identified [35]. Many amyloidogenic peptides contain Arg and Lys residues and have cell attachment activity. The Arg and Lys residues may contribute to cellular effects as a basic cluster in the fibrils. The FVFYV peptide assembles itself and forms amyloid-like fibrils without cellular effects and is easily modified with functional sequences. FVFYV is useful to apply as a core sequence for designing functional amyloid-like fibrils.

CONCLUSION

This Ph.D. dissertation is entitled “Structural Requirement of hA5G18 Peptide (DDFVFYVGGYPS) from Laminin α5 Chain for Amyloid-like Fibril Formation and Cell Adhesion”. It describes the discovery of structural requirements for the hA5G18 peptide and the relationship between the amyloid-like fibril formation and cell attachment activity.

Basement membranes play physical and biological roles in the tissues. Recombinant proteins and synthetic peptides derived from basement membranes are particularly important as biomaterials especially in the perspective of regenerative medicine [1, 2]. Laminin is the major component of the basement membrane for the biological activity. It is a heterotrimeric glycoprotein with a cruciform structure composed of three subunits: α, β, and γ chains [3-5]. To date, five α laminin chains (α1-α5), three β chains (β1-β3), and three γ chains (γ1-γ3) have been identified, and α chain in a different place plays an essential role in diverse biological functions of laminins. It is expressed in a tissue- and developmental stage-specific manner, and there are at least 19 different laminins isoform have been discovered by various combinations of each subunit [5]. The G domain located at the C-terminus of the laminin chain consists of α5 LG modules (LG1-LG5) and plays an essential role in the expression of various functions of laminin [3-5].

Amyloid fibrils are in many cases observed to interact with cells and are often related to diseases. Here, I focused on the amyloid-like fibril formation of laminin peptide fragments. The amyloid fibril formation of degraded proteins is often related to diseases such as Alzheimer’s disease, type II diabetes, Parkinson’s disease, prion diseases, and systemic polyneuropathies [6–8]. Identifying amyloidogenic peptides leads to a better understanding of the mechanism of disease.

Previously, Kumai et al. screened biologically active sequences in the human laminin α5 chain G domain using 115 synthetic peptides by the peptide-coated plate and peptide-conjugated chitosan matrix assays [27]. The results suggested that two peptides, hA5G18 and hA5G26, aggregate on the plastic plates and promote cell adhesion, but the aggregation mechanism has not been identified.

Therefore, in this paper, in chapter 1, I focus on these two peptides, hA5G18 and hA5G26. I describe how hA5G18 forms amyloid-like fibrils and how hA5G26 didn't show amyloid-like fibrils formation activity through the Congo red staining assay and the electron microscopic analysis, and the peptide-coated plate assay and Sepharose beads assay showed that hA5G18 was active in the peptide-coated plate assay but inactive in the Sepharose beads assay. These

results indicated that amyloid-like fibril formation is required for the cell attachment activity of hA5G18. The deletion analysis showed that hA5G18BTC5 (FVFYV) is the minimal essential sequence for amyloid-like fibril formation, but it is inactive in cell attachment. The Congo red staining assay and the cell attachment activity assay of the Alanine-substituted hA5G18B peptide also showed that the Phe1, Val2, Phe3, and Tyr4 residues are critical for cell attachment activity. This proves the importance of FVFYV for hA5G18B amyloid fibril formation activity from another aspect. I can also conclude that FVFYV has the potential to be used as the core sequence for amyloid fibrils.

Further, in chapter 2, I designed a functional amyloid-like fibril using an integrin αvβ3 binding sequence RGD and FVFYV with GG as a spacer, and the sequence FVFYVGGRGE has been designed as the negative control. I conducted an EDTA heparin inhibition assay and antibody inhibition assay on these two peptides. The results suggest that the RGD conjugated the FVFYV peptide FVFYVGGRGD and the negative control FVFYVGGRGE formed amyloid-like fibrils and similarly promoted cell attachment. Moreover, the cell adhesion and spreading activities of the peptides were not influenced by the anti-integrin αvβ3 antibody but were inhibited by the anti-integrin β1 antibody. These results suggest that RGD and RGE contribute similarly to the fibrils. Therefore, I hypothesized that Arginine residues might be involved in the cell attachment activity.

Previously basic amino acids in amyloidogenic peptides were described to be essential for cell attachment activity through HSPGs, such as syndecans [13,14]. I conjugated basic amino acids (Arg, Lys, and His) to the FVFYV peptide with GG as a spacer and examined their activity by Congo red staining assay and cell attachment assay. The result suggests that FVFYVGGR and FVFYVGGK promoted cell attachment activity, but FVFYVGGH did not. These results indicated that His residue is weakly basic and does not contribute to the activity. Additionally, FVFYVGGR and FVFYVGGK promote integrin-mediated cell attachment. These results suggest that Arg and Lys residues promote cellular effects when they are incorporated-like in amyloid, polymerized basic amino acids, such as poly-R, promoting integrin β1-mediated cell adhesion similar to that of FVFYVGGR and FVFYVGGK. The cell attachment of poly-R was completely inhibited by heparin and weakly inhibited by the EDTA and antiβ1-integrin antibody. However, the cell spreading of poly-R was completely inhibited by the anti-integrin β1 antibody. Since poly-R is highly basic and interacts strongly with HSPG, it may not be easy to find the effect of EDTA and the anti-integrin β1 antibody. Polymerized basic amino acids in polymers or fibrils have the potential to interact with heparin and integrin β1 [19]. Various amyloidogenic peptides have previously been identified [13]. Amyloidogenic peptides contain Arg and Lys residues and have cell attachment activity. The Arg and Lys residues may contribute to cellular

effects as a basic cluster in the fibrils.

Further, I tried to figure out whether FVFYV promotes the same amyloid-like fibril formation activity in other peptides containing the FVFYV sequence. In a previous experiment, A5G15 showed the same experimental result of the FVFYV sequence obtained from current study. Because I found the FVFYV sequence in the human laminin α5 chain G domain, and the homology between mouse laminin α5 chain and human laminin α5 chain peptide sequence is about 79% [25,26], and hA5G178 which is corresponding to the A5G15 peptide in the human laminin α5 chain G domain. The result of the Congo red staining assay and cell attachment assay suggest that the minimal essential sequence for amyloid-like fibril formation activity is PDDFVFY, and the minimal essential sequence for cell attachment activity is RPDDFVFY. This is different from our previous results, it might be because the Proline residue and Aspartic Acid residue promote a hydrophilic side chain, and the hydrophobic side chain of Valine residue has been removed, which makes the whole peptide sequence exhibited hydrophobicity. Hence, it affects the activity of this particular sequence for the amyloid-like fibril formation activity. PDDFVFYV may have higher amyloid-like fibril formation activity than FVFYV. But this result can only be considered as an individual case.

In summary, hA5G18B (FVFYVGGYPS) is the minimum sequence for amyloid-like fibril formation and cell attachment. The Ala-substitution analysis of hA5G18B suggests that the Pro residue is critical for the cell spreading activity of hA5G18B. However, the mechanism of Pro is unclear at this time. These results suggest that sequences other than basic amino acids may be active in amyloid fibrils. FVFYV is helpful to apply as a core sequence for designing functional amyloid-like fibrils and has the potential for use as a unique platform for a cell scaffold material.

Self-assembling amyloidogenic peptides are easily modified with biologically active ligands, including peptides, and functional amyloid-like fibrils have been used as a biomaterial [37, 68]. The FVFYV peptide assembles itself, forms amyloid-like fibrils without cellular effects, and is easily modified with functional sequences. FVFYV is useful to apply as a core sequence for designing functional amyloid-like fibrils and has the potential for use as a unique platform for a cell scaffold material.

EXPERIMENTAL PARTS

1. Materials and Methods

1.1. Synthetic peptides

All peptides were synthesized by the 9-fluorenylmethoxycarbonyl (Fmoc) based solid-phase method. The Rink amide resin ((4,2,4-dimethoxyphenyl-Fmoc-aminomethyl)-phenoxy resin) was used for peptide synthesis, synthesized with an amide at the C-terminal, and the resin was weighed at a 50 μmol scale. Side chain protecting groups are trityl group for Asn, Cys, Gln, and His, t-butyl group for Asp, Glu, Ser, Thr, and Tyr, and 2,2,5,7,8-pentamethylchroman-6-sulfonyl group for Arg, Lys with a t-butoxycarbonyl group was used (Novabiochem, San Diego, CA, and Watanabe Chem, Hiroshima, Japan).

The weighted resin was placed in the PD-10 column (Cytiva, Tokyo, Japan) and washed three times with *N, N*-dimethylformamide (DMF, Kanto Kagaku), after that, resin deprotection of the Fmoc group to the resin was carried out by adding 20% piperidine containing DMF and shaking for 15 min at room temperature. The resin was washed three times with DMF, then, washed resin was reacted with condensing agents, and the Fmoc-protected amino acid dissolved in DMF for 1 hr condensation reaction. the condensing agents are *N, N'*-Diisopropylcarbodiimide (DIC, Kokusan Kagaku)/Hydroxybenzotriazole (HOBt, Watanabe Kagaku). After condensation, the completion of the reaction was confirmed by the Kaiser test using ninhydrin. After completion of the reaction, the amino acid-loaded resin was washed three times with DMF. Following, the Fmoc group was again deprotected with 20% piperidine/DMF for 20 min, after that, the same operation is repeated. Finally, the resulting protected peptide-resin was washed with methanol three times, diethyl ether three times, and air-dried. Next, trifluoroacetic acid (TFA, Kanto Chemical): thioanisole (Tokyo Kasei): m-cresol (Tokyo Kasei): ethane-1,2-dithiol (Tokyo Kasei): ultrapure water (80:5:5:5:5, v/v/v/v/v) mixture was added into the resin, and shaken at room temperature for 3 hrs to deprotect the side chain protecting groups and remove the peptide from the resin. The solution was filtered using a 0.45-micron nylon membrane (Iwaki Co. Ltd., Tokyo, Japan), a filtrate containing the peptide was obtained. Chilled diethyl ether was added to the filtrate to precipitate the peptide, which was collected by centrifugation. The precipitate was washed again with diethyl ether and centrifuged in the same manner. This operation was repeated three times, and the precipitate was air-dried at room temperature. Add an appropriate amount of 50% acetic acid/Mill-Q water to dissolve (crude peptide), the crude peptides were purified by reversed phase HPLC using Mightysil RP-18 GP 250-20 column (Kanto Chemical Co., Inc., Tokyo, Japan) with a binary solvent system (0.1%

TFA in acetonitrile and 0.1% TFA in Mill-Q water). The purified peptides solutions were lyophilized and obtained purified peptide as white feathery powders. Purity and mass of the peptides were confirmed by an analytical HPLC and an electrospray ionization mass spectrometer at the Central Analysis Center, Tokyo University of Pharmacy and Life Sciences.

hA5G26: H-Leu-Asp-Gly-Thr-Gly-Phe-Ala-Arg-Ile-Ser-Phe-Asp-NH_2
HRMS(ES+) m/z calculated for $C_{58}H_{88}N_{16}O_{18}$ $[M+H]^+$ 1297.6541, found in 1297.6528

hA5G18: H-Asp-Asp-Phe-Val-Phe-Tyr-Val-Gly-Gly-Tyr-Pro-Ser-NH_2
HRMS(ES+) m/z calculated for $C_{66}H_{85}N_{13}O_{19}$ $[M+H]^+$ 1364.6163, found in 1364.6150

hA5G18A: H-Asp-Phe-Val-Phe-Tyr-Val-Gly-Gly-Tyr-Pro-Ser-NH_2
HRMS(ES+) m/z calculated for $C_{62}H_{80}N_{12}O_{16}$ $[M+H]^+$ 1249.5893, found in 1249.5883

hA5G18B: H-Phe-Val-Phe-Tyr-Val-Gly-Gly-Tyr-Pro-Ser-NH_2
HRMS(ES+) m/z calculated for $C_{58}H_{75}N_{11}O_{13}$ $[M+H]^+$ 1134.5624, found in 1134.5614

hA5G18C: H-Val-Phe-Tyr-Val-Gly-Gly-Tyr-Pro-Ser-NH_2
HRMS(ES+) m/z calculated for $C_{49}H_{66}N_{10}O_{12}$ $[M+H]^+$ 987.4940, found in 987.4899

hA5G18BTC1: H-Phe-Val-Phe-Tyr-Val-Gly-Gly-Tyr-Pro-NH_2
HRMS(ES+) m/z calculated for $C_{55}H_{70}N_{10}O_{11}$ $[M+H]^+$ 1047.5304, found in 1047.5282.

hA5G18BTC2: H-Phe-Val-Phe-Tyr-Val-Gly-Gly-Tyr-NH_2
HRMS(ES+) m/z calculated for $C_{50}H_{63}N_9O_{10}$ $[M+H]^+$ 950.4776, found in 950.4774

hA5G18BTC3: H-Phe-Val-Phe-Tyr-Val-Gly-Gly-NH_2
HRMS(ES+) m/z calculated for $C_{41}H_{54}N_8O_8$ $[M+H]^+$ 787.4143, found in 787.4146.

hA5G18BTC4: H-Phe-Val-Phe-Tyr-Val-Gly-NH_2
HRMS(ES+) m/z calculated for $C_{39}H_{51}N_7O_7$ $[M+H]^+$ 730.3928, found in 730.3934.

hA5G18BTC5: H-Phe-Val-Phe-Tyr-Val-NH_2
HRMS(ES+) m/z calculated for $C_{37}H_{48}N_6O_6$ $[M+H]^+$ 673.3714, found in 673.3717.

hA5G18BTC6: H-Phe-Val-Phe-Tyr-NH_2
HRMS(ES+) m/z calculated for $C_{32}H_{39}N_5O_5$ $[M+H]^+$ 574.3029, found in 574.3031.

hA5G18BA1: H-Ala-Val-Phe-Tyr-Val-Gly-Gly-Tyr-Pro-Ser-NH_2
HRMS(ES+) m/z calculated for $C_{52}H_{71}N_{11}O_{13}$ $[M+H]^+$ 1058.5311, found in 1058.5306.

hA5G18BA2: H-Phe-Val-Phe-Tyr-Val-Gly-Gly-Tyr-Pro-Ser-NH_2
HRMS(ES+) m/z calculated for $C_{56}H_{71}N_{11}O_{13}$ $[M+H]^+$ 1106.5311, found in 1106.5309.

hA5G18BA3: H-Phe-Val-Phe-Tyr-Val-Gly-Gly-Tyr-Pro-Ser-NH_2
HRMS(ES+) m/z calculated for $C_{52}H_{71}N_{11}O_{13}$ $[M+H]^+$ 1058.5311, found in 1058.5306.

hA5G18BA4: H-Phe-Val-Phe-Tyr-Val-Gly-Gly-Tyr-Pro-Ser-NH_2
HRMS(ES+) m/z calculated for $C_{52}H_{71}N_{11}O_{12}$ $[M+H]^+$ 1042.5362, found in 1042.5363.

hA5G18BA5: H-Phe-Val-Phe-Tyr-Val-Gly-Gly-Tyr-Pro-Ser-NH_2
HRMS(ES+) m/z calculated for $C_{56}H_{71}N_{11}O_{13}$ $[M+H]^+$ 1106.5311, found in 1106.5313.

hA5G18BA6: H-Phe-Val-Phe-Tyr-Val-Gly-Gly-Tyr-Pro-Ser-NH_2
HRMS(ES+) m/z calculated for $C_{59}H_{77}N_{11}O_{13}$ $[M+H]^+$ 1148.5781, found in 1148.5781.

hA5G18BA7: H-Phe-Val-Phe-Tyr-Val-Gly-Gly-Tyr-Pro-Ser-NH_2
HRMS(ES+) m/z calculated for $C_{59}H_{77}N_{11}O_{13}$ $[M+H]^+$ 1148.5781, found in 1148.5776.

hA5G18BA8: H-Phe-Val-Phe-Tyr-Val-Gly-Gly-Tyr-Pro-Ser-NH_2
HRMS(ES+) m/z calculated for $C_{52}H_{71}N_{11}O_{12}$ $[M+H]^+$ 1042.5362, found in 1042.5360.

hA5G18BA9: H-Phe-Val-Phe-Tyr-Val-Gly-Gly-Tyr-Pro-Ser-NH_2
HRMS(ES+) m/z calculated for $C_{56}H_{73}N_{11}O_{13}$ $[M+H]^+$ 1108.5468, found in 1108.5464.

hA5G18BA10: H-Phe-Val-Phe-Tyr-Val-Gly-Gly-Tyr-Pro-Ser-NH_2
HRMS(ES+) m/z calculated for $C_{58}H_{75}N_{11}O_{12}$ $[M+H]^+$ 1118.5675, found in 1118.5669.

FVFYVGGRGD: H-Phe-Val-Phe-Tyr-Val-Gly-Gly-Arg-Gly-Asp-NH_2
HRMS(ES+) m/z calculated for $C_{53}H_{74}N_{14}O_{13}$ $[M+H]^+$ 1115.5638, found in 1115.5634.

FVFYVGGRGE: H-Phe-Val-Phe-Tyr-Val-Gly-Gly-Arg-Gly-Glu-NH_2
HRMS(ES+) m/z calculated for $C_{54}H_{76}N_{14}O_{13}$ $[M+H]^+$ 1129.5795, found in 1129.5788.

FVFYVGGR: H-Phe-Val-Phe-Tyr-Val-Gly-Gly-Arg-NH_2
HRMS(ES+) m/z calculated for $C_{47}H_{66}N_{12}O_9$ $[M+H]^+$ 943.5154, found in 943.5156.

FVFYVGGK: H-Phe-Val-Phe-Tyr-Val-Gly-Gly-Lys-NH_2
HRMS(ES+) m/z calculated for $C_{47}H_{66}N_{10}O_9$ $[M+H]^+$ 915.5092, found in 915.5094.

FVFYVGGH: H-Phe-Val-Phe-Tyr-Val-Gly-Gly-His-NH_2
HRMS(ES+) m/z calculated for $C_{47}61N_{11}O_9$ $[M+H]^+$ 924.4732, found in 924.4731.

RGGFVFYV: H-Arg-Gly-Gly-Phe-Val-Phe-Tyr-Val-NH_2
HRMS(ES+) m/z calculated for $C_{47}H_{66}N_{12}O_9$ $[M+H]^+$ 943.5154, found in 943.5157.

hA5G178TC1: **H-Arg-Pro-Asp-Asp-Phe-Val-Phe-Tyr-Val-Gly-Gly-NH_2**
HRMS(ES+) m/z calculated for $C_{60}H_{83}N_{15}O_{16}$ $[M+H]^+$ 1270.6220, found in 1270.6221.

hA5G178TC2: **H-Arg-Pro-Asp-Asp-Phe-Val-Phe-Tyr-Val-Gly-NH_2**
HRMS(ES+) m/z calculated for $C_{58}H_{80}N_{14}O_{15}$ $[M+H]^+$ 1213.6006, found in 1212.6010.

hA5G178TC3: **H-Arg-Pro-Asp-Asp-Phe-Val-Phe-Tyr-Val-NH_2**
HRMS(ES+) m/z calculated for $C_{56}H_{77}N_{13}O_{14}$ $[M+H]^+$ 1156.5791, found in 1156.5793.

hA5G178TC4: **H-Arg-Pro-Asp-Asp-Phe-Val-Phe-Tyr-NH_2**
HRMS(ES+) m/z calculated for $C_{51}H_{68}N_{12}O_{13}$ $[M+H]^+$ 1057.5107, found in 1057.5106.

hA5G178TC5: **H-Arg-Pro-Asp-Asp-Phe-Val-Phe-NH_2**
HRMS(ES+) m/z calculated for $C_{42}H_{59}N_{11}O_{11}$ $[M+H]^+$ 894.4474, found in 894.4476.

hA5G178TC6: **H-Arg-Pro-Asp-Asp-Phe-Val-NH_2**
HRMS(ES+) m/z calculated for $C_{33}H_{50}N_{10}O_{10}$ $[M+H]^+$ 747.3790, found in 747.3788.

hA5G178TN1TC4: **H-Pro-Asp-Asp-Phe-Val-Phe-Tyr-NH_2**
HRMS(ES+) m/z calculated for $C_{45}H_{56}N_8O_{12}$ $[M+H]^+$ 901.4096, found in 901.4095.

hA5G178TN2TC4: **H-Asp-Asp-Phe-Val-Phe-Tyr-NH_2**
HRMS(ES+) m/z calculated for $C_{40}H_{49}N_7O_{11}$ $[M+H]^+$ 804.3568, found in 804.3574.

hA5G178TN3TC4: **H-Asp-Phe-Val-Phe-Tyr-NH_2**
HRMS(ES+) m/z calculated for $C_{36}H_{44}N_6O_6$ $[M+H]^+$ 689.3299, found in 689.3300.

1.2. Antibodies

Rat monoclonal antibody against human integrin α6 (P5G10) was purchased from AMAC (Westbrook, ME, USA). Mouse monoclonal antibodies against human integrin αvβ3 (VNR-1), α3 (P1B5), β1 (AIIB2), and α2β1 (VLA-2) were purchased from Millipore Co. Ltd. (Billerica, MA, USA). Mouse monoclonal antibody against human IgG heavy chain (MR36G) was purchased from Sigma-Aldrich (St. Louis, MO, USA).

1.3. Congo red binding analysis

To make a 100 μM Congo red stock solution, Congo red was dissolved in 10% ethanol containing phosphate-buffered saline (PBS). 10% methanol was added to prevent micelle formation of Congo red and filtered three times using a 0.45-micron nylon membrane (Iwaki Co. Ltd., Tokyo, Japan). Each of the peptide solutions (0.1 mM, 100 μL) in Mill-Q water and the Congo red stock solution (100 μL) were mixed with 800 μL of PBS (1.25x) and placed in disposable cuvettes for 24 hrs at room temperature in the dark. After incubation for 24 hrs, absorption spectra were measured from 300 to 700 nm using a UV-1700 UV/Vis spectrophotometer (Shimadzu Co. Ltd., Kyoto, Japan).

1.4. Transmission electron microscopy (TEM)

Peptide solution (1 mM) was diluted 1:0 to 1:4 in Milli-Q water and applied onto a grid mesh with carbon-coated Formvar film (Okenshoji Co. Ltd., Tokyo, Japan). The specimen was

negatively stained with a 2% aqueous solution of phosphotungstic acid and observed using JEM-1011 (JEOL Ltd., Tokyo, Japan) electron microscope at an acceleration voltage of 80 kV.

1.5. Cells and culture

Human neonatal dermal fibroblasts (HDFs) (AGC Techno Glass Co., Ltd., Chiba, Japan) were maintained in low glucose containing Dulbecco's modified Eagle's medium (DMEM; Invitrogen, Carlsbad, CA, USA) with 10% fetal bovine serum (FBS, Invitrogen), 100 U/mL penicillin, and 100 μg/mL streptomycin (Invitrogen) under 37 °C in a humidified, 5% CO_2 atmosphere.

1.6. Preparation of peptide-coated plate

Peptide-coated plates were created using 96-well plates (Nunc). Synthetic peptides were prepared to a concentration of 1 mM using Mill-Q water. Peptide solutions diluted to various concentrations were added to each well (100 μL/well) and air-dried at room temperature for more than 24 hrs to prepare peptide-coated plates.

1.7. Cell attachment assay using peptide-coated plates

96-well Plates (Nunc, Inc., Naperville, IL, USA) were coated with various amounts of peptides in water and dried over at room temperature. After washing three times with PBS, the peptide-coated wells were blocked with 1% bovine serum albumin (BSA; Sigma, St. Louis, MO, USA) in DMEM (150 μL) for 1 hr, then the plates were washed twice with DMEM containing 0.1% BSA (100 μL). Cells were detached by 0.05% trypsin/ethylenediaminetetraacetic acid (EDTA) and detached HDFs were suspended in a medium containing 10% FBS/1% penicillin/1% streptomycin and incubated at 37°C and 5% CO_2 for 20 min, then washed twice with 0.1% BSA/DMEM. After that, HDFs were resuspended in 0.1% BSA/DMEM, seeded at 100 μL per well (2×10^4 cells/well), and incubated at 37°C, 5% CO_2 for 1 hr. The attached cells were stained with 0.2% crystal violet aqueous solution containing 20% methanol (100 μL) for 10 min at room temperature. After washing several times with water and air-dried, the attached cells were photographed using a BZ-X810 microscope (Keyence, Osaka, Japan). Images were analyzed using BZ-analyzer software (Keyence). The attached cells in three randomly selected fields were counted. Each experiment was repeated at least three times.

1.8. Inhibition evaluation of anti-integrin antibody against cell adhesion using peptides

96-well plates were coated with peptides as described above. Poly-L-arginine

hydrochloride (molecular weight > 70,000) was dissolved in Mill-Q water (final concentration of 2 mM) (100 μL/well) and coated and dried over at room temperature. Various anti-integrin antibodies were added to the cell suspension at concentrations of 10 μg/mL of the anti-αvβ3, α3/α6, β1 integrin antibodies and 30 μg/mL of the anti-α2β1 integrin antibody. and incubated at room temperature for 15 mins, 100 μL of cell suspension was added to each well (2×10^4 cells/well) and incubated for 1 hr at 37°C and 5% CO_2. After incubation, 0.2% crystal violet/20% methanol aqueous solution (100 μL) was added to stain adherent cells for 15 min, and the plate was washed twice with Mill-Q water, after air-dried, the plate was imaged by the BZ-X810 microscope. and the number of adherent cells was counted in the same manner as the cell adhesion activity evaluation described above.

1.9. Inhibition evaluation of heparin and EDTA on cell adhesion using peptides

96-well plates were coated with peptides as described above. Poly-L-arginine hydrochloride (molecular weight>70,000) was dissolved in Mill-Q water (final concentration of 2 mM) (100 μL/well) and coated and dried over at room temperature. 10 μg/mL heparin and 5 mM EDTA were mixed with the cell suspension. 100 μL of cell suspension was added to each well (2×10^4 cells/well) and incubated for 1 hr at 37°C and 5% CO_2. After incubation, 0.2% crystal violet/20% methanol aqueous solution (100 μL) was added to stain adherent cells for 15 min, and the plate was washed twice with Mill-Q water, after air-dried, the plate was imaged by the BZ-X810 microscope. and the number of adherent cells was counted in the same manner as the cell adhesion activity evaluation described above.

1.10 Cell attachment assay using peptide-conjugated Sepharose beads

The synthetic peptides were coupled to cyanogen bromide (CNBr)-activated Sepharose 4B (GE Healthcare, London, UK) beads as described previously13. First, the CNBr-activated Sepharose 4B beads were powdered by 0.1 M acetate buffers (pH 4.0) containing 0.5 M NaCl (hereinafter referred to as Buffer A) for 1 hr at room temperature, and the peptides (200μg) were dissolved in 1 mL of 0.1 M NaHCO3 solutions containing 0.5 M NaCl (pH 8.3) (hereinafter referred to as Buffer B) to obtained peptide solution. The CNBr-activated Sepharose beads (30 mg) were incubated with the peptide solution for overnight at 4°C. After incubation, beads were washed with 1 mL of Buffer B for 5 times. Then, unreacted CNBr residues were quenched with 1 M ethanolamine (pH 8.0) for 2 hrs at room temperature, three cycles of washing are performed in the order of Buffer B and then Buffer A. After washed, the peptide-conjugated Sepharose beads were stocked in the PBS (-). AG73-coupled beads and ethanolamine-coupled beads were prepared as a positive and negative control.

The HDF cells were resuspended in 0.1% BSA containing DMEM (1 x 10^5 cells/100 μL) and incubated with 3 mg/50 μL peptide-beads solution in the tube for 1 hr at 37 °C. After incubation, carefully aspirate the supernatant, add 0.2% crystal violet aqueous solution in 20% methanol as stain and transfer the solution to the 24-wells plate to separate individual cell attachment Sepharose beads. After washed for three times with Mill-Q, the cell attachment Sepharose beads were observed under a BZ-X810. Each assay was repeated at least twice.

1.11 Evaluation of cell morphology using peptides

According to the method described above, a peptide-coated plate and cells were prepared. 100 L of resuspended HDFs were seeded in each well (1×10^4 cells/well) and incubated at 37°C, 5% CO_2 for 2 hrs. After incubation, 0.2% crystal violet/20% methanol aqueous solution (100 μL) was added to stain adherent cells for 15 min, and the plate was washed twice with ultrapure water. Adhered cells were photographed using a BZ-X810 microscope (Keyence, Osaka, Japan). Images were analyzed using BZ-analyzer software (Keyence). The attached cells in three randomly selected fields were counted. Each experiment was repeated at least three times.

1.12 Statistics Analysis

Results were expressed as ± standard deviation (S.D.). Comparison of mean values was performed using one-way analysis of variance, and a homoscedastic *t* test. $P<0.05$ indicated statistical significance.

REFERENCES

1. Yurchenco, P. D., Schittny, J. C., *FASEB J.*, **4**, 1577-1590 (1990).
2. Kruegel, J., Miosge, N., *Cell. Mol. Life Sci.*, **67**, 2879-2895 (2010).
3. Scheele, S., Nystrom, A., Durbeej, M., Talts, J. F., Ekblom, M., Ekblom, P., *J. Mol. Med. (Berl).*, **85**, 825-836 (2007).
4. Miner, J. H., *Microsc. Res. Techr.*, **71**, 341-359 (2008).
5. Durbeej, M., *Cell Tissue Res.*, **339**, 259-268 (2010).
6. Colognato, H., and Yurchenco, P. D., *Dev. Dyn.*, **218**, 213-234 (2000).
7. Yamada, K. M., *J. Biol. Chem.*, **270**, 12809-12812 (1991).
8. Yamada, Y. and Kleinman, H. K., *Curr. Opin. Cell Biol.*, **4**, 819-823 (1992).
9. Nomizu, M., Kim, W. H., Yamamura, K., Utani, A., Song, S. Y., Otaka, A., Roller, P. P., Kleinman, H. K., and Yamada, Y., *J. Biol. Chem.*, **270**, 20583-20590 (1995).
10. Hozumi, K., Ishikawa, M., Hayashi, T., Yamada, Y., Katagiri, F., Kikkawa, Y., Nomizu, M., *J Biol Chem.*, **287**, 25111-22 (2012).
11. Negishi, Y., Nomizu, M., *Pharmacol. Ther.*, **202**, 91-97 (2019).
12. Makino, M., Okazaki, I., Nishi, N., and Nomizu, M., *Connect. Tissue.*, **31**, 227-234 (1999).
13. Nomizu, M., Kuratomi, Y., Song, S. Y., Ponce, L. M., Hoffman, M. P., Powell, S. K., Miyoshi, K., Otaka, A., Kleinman, H. K., and Yamada, Y., *J. Biol. Chem.*, **272**, 32198-32205 (1997).
14. Nomizu, M., Kuratomi, Y., Malinda, M. K., Song, S. Y., Miyoshi, K., Otaka, A., Powell, S. K., Hoffman, M. P., Kleinman, H. K., and Yamada, Y., *J. Biol. Chem.*, **273**, 32491-32499 (1998).
15. Nomizu, M., Kuratomi, Y., Ponce, L. M., Song, S. -Y., Miyoshi, K., Otaka, A., Powell, S. K., Hoffman, M. P., Kleinman, H. K., and Yamada, Y., *Arch. Biochem. Biophys.*, **378**, 311-320 (2000).
16. Suzuki, N., Yokoyama, F., and Nomizu, M., *Connect. Tissue Res.*, 46, 142-152 (2005).
17. Timpl, R., Tisi, D., Talts, J. F., Andac, Z., Sasaki, T., and Hohenester, E., *Matrix Biol.*, **19**, 309-317 (2000).
18. Weeks, B. S., Nomizu, M., Ramchandran, R. S., Yamada, Y., Kleinman, H. K., *Exp. Cell Res.*, **243**, 375-382 (1998).
19. Hoffman, M. P., Engbring, J. A., Nielsen, P. K., Vargas, J., Steinberg, Z., Karmand, A. J., Nomizu, M., Yamada, Y., Kleinman, H. K., *J. Biol. Chem.*, **276**, 22077-22085 (2001).
20. Hayashi, K., Mochizuki, M., Nomizu, M., Uchinuma, E., Yamashina, S., Kadoya, Y., *J.*

Invest. Dermatol., **118**, 712-718 (2002).

21. Ponce, M. L., Hibino, S., Lebioda, A. M, Mochizuki, M., Nomizu, M., Kleinman, H. K., *Cancer Res.*, **63**, 5060-5064 (2003).
22. Suzuki, N., Nakatsuka, H., Mochizuki, M., Nishi, N., Kadoya, Y., Utani, A., Oishi, S., Fujii, N., Kleinman, H. K., Nomizu, M., *J. Biol. Chem.*, **278**, 45697-45705 (2003).
23. Hozumi, K., Suzuki, N., Nielsen, P. K., Nomizu, M., and Yamada, Y., *J. Biol. Chem.*, **281**, 32929-32940 (2006).
24. Makino, M., Okazaki, I., Kasai, S., Nishi, N., Bougaeva, M., Weeks, B. S., Otaka, A., Nielsen, P. K., Yamada, Y., Nomizu, M., *Exp. Cell Res*., **277**, 95-106, (2002)
25. Miner, J. H., Lewis, R. M., Sanes, J. R., *J. Biol. Chem.*, **270**, 28523-28526 (1995)
26. Doi, M., Thyboll, J., Kortesmaa, J., Jansson, K., Iivanainen, A., Parvardeh, M., Timpl, R., Hedin, U., Swedenborg, J., Tryggvason, K., *J. Biol. Chem.*, **277**, 12741-8 (2002)
27. Kumai, J., Yamada, Y., Hamada, K., Katagiri, F., Hozumi, K., Kikkawa, Y., Nomizu, M., *J. Pept. Sci.*, **25**, e3218 (2019).
28. Guijarro, J. I., Sunde, M., Jones, J. A., Campbell, I. D., and Dobson, C. M., *Proc. Natl. Acad. Sci. U.S.A.*, **95**, 4224-4228 (1998).
29. Kelly, J.W., *Curr. Opin. Struct. Biol.*, **8**, 101–106 (1998).
30. Rochet, J.C., Lansbury, P.T. Jr., *Curr. Opin. Struct. Biol*., **10**, 60–68 (2000).
31. Katagiri, F., Ueo, D., Okubo-Gunge, Y., Usui, A., Kuwatsuka, S., Mine, Y., Hamada, K., Fujiwara, S., Sasaki, T., Nomizu, M., Utani, A., *JID Innov.*, **2**, 100114 (2022).
32. Berhanu, W.M., Hansmann, U.H. *PLoS ONE.*, **7**, e41479 (2012).
33. Chiti, F., Dobson, C.M., *Annu. Rev. Biochem.*, **75**, 333–366 (2006).
34. Dobson, C.M. *Cold Spring Harb Perspect. Biol.*, **9**, a023648 (2017).
35. Kasai, S., Urushibata, S., Hozumi, K., Yokoyama, F., Ichikawa, N., Kadoya, Y., Nishi, N., Watanabe, N., Yamada, Y., Nomizu, M., *Biochemistry.*, **46**, 3966–3974 (2007).
36. Katagiri, F., Takeyama, K., Ohga, Y., Hozumi, K., Kikkawa, Y., Kadoya, Y., Nomizu, M., *Biochemistry.*, **49**, 5909–5918 (2010).
37. Ohga, Y., Katagiri, F., Takeyama, K., Hozumi, K., Kikkawa, Y., Nishi, N., Nomizu, M., *Biomaterials.*, **30**, 6731–6738 (2009).
38. Miner, J.H., Cunningham, J., Sanes, J.R., *J. Cell Biol.*, **143**, 1713–1723 (1998).
39. Miner, J.H., Li, C., *Dev. Biol.*, **217**, 278–289 (2000).
40. Bolcato-Bellemin, A.L., Lefebvre, O., Arnold, C., Sorokin, L., Miner, J.H., Kedinger, M., Simon-Assmann, P., *Dev. Biol.*, **260**, 376–390 (2003).
41. Kikkawa, Y., Virtanen, I., Miner, J.H., Lin HB., *J. Cell Biol.*, **161**, 187–196 (2003).
42. Kikkawa, Y., Sanzen, N., Sekiguchi, K., *J. Biol. Chem.*, **273**, 15854–15859 (1998)

43. Kikkawa, Y., Sanzen, N., Fujiwara, H., Sonnenberg, A., and Sekiguchi, K., *J. Cell Sci.*, **113**, 869–876 (2000).
44. Shimizu, H., Hosokawa, H., Ninomiya, H., Miner, J. H., Masaki, T., *J. Biol. Chem.*, **274**, 11995–12000 (1999).
45. El Nemer, W., Gane, P., Colin, Y., Bony, V., Rahuel, C., Galacteros, F., J. P., and Le Van Kim, C., *J. Biol. Chem.*, **273**, 16686–16693 (1998).
46. Udani, M., Zen, Q., Cottman, M., Leonard, N., Jefferson, S., Daymont, C., Truskey, G., Telen, M. J., *J. Clin. Invest.*, **101**, 2550–2558 (1998).
47. Kikkawa, Y., Moulson, C. L., Virtanen, I., Miner, J. H. *J. Biol. Chem.*, **277**, 44864–44869 (2002).
48. Sipe, J. D., Cohen, A. S., *J. Struct. Biol.*, **130**, 88-98 (2000).
49. Katagiri, F., Ohga, Y., Takeyama, K., Hozumi, K., Kikkawa, Y., Kadoya, Y., Nomizu, M., *Arch. Biochem. Biophys.*, **500**, 189–195 (2010).
50. Morrison KL, Weiss GA., *Curr Opin Chem Biol.*, **5**, 302–7 (2001).
51. Weiss GA, Watanabe CK, Zhong A, Goddard A, Sidhu SS. *Proc. Natl. Acad. Sci. U.S.A.*, **97**, 8950–4 (2000).
52. Anderson DG, Burdick JA, Langer R., *Science.*, **305**, 1923–4 (2004).
53. Semino CE. *J Biomed Bio-technol.*, **2003**, 164–9 (2003).
54. Lutolf MP, Hubbell JA. *Nat Biotechnol.*, **23**, 47–55 (2005).
55. Hersel U, Dahmen C, Kessler H., *Biomaterials.*, **24**, 4385–415 (2003).
56. Genove E, Shen C, Zhang S, Semino CE., *Biomaterials.*, **26**, 3341–51 (2005).
57. Dunehoo AL, Anderson M, Majumdar S, Kobayashi N, Berkland C, Siahaan TJ., *J Pharm Sci.*, **95**, 1856–72 (2006).
58. Akiyama SK., *Hum Cell.*, **9**, 181–6 (1996).
59. Miyazaki, T., Futaki, S., Suemori, H., Taniguchi, Y., Yamada, M., Kawasaki, M., Hayashi, M., Kumagai, H., Nakatsuji, N., Sekiguchi, K., Kawase, E., *Nat. Commun.*, **3**, 1236 (2012).
60. E Ruoslahti. *Annu Rev Cell Dev Biol.*, **12**, 697-715 (1996).
61. Lin HB., Garciaecheverria C., Asakura S., Sun W., Mosher DF., Cooper SL., *Biomaterials.*, **13**, 905–14 (1992).
62. Hilbich, C., Kisters-Woike, B., Reed, J., Masters, C. L., and Beyreuther, K., *J. Mol. Biol.*, **228**, 460-473 (1992).
63. Suzuki, N., Nakatsuka, H., Mochizuki, M., Nishi, N., Kadoya, Y., Utani, A., Oishi, S., Fujii, N., Kleinman, H.K., Nomizu, M., *J. Biol. Chem.*, **278**, 45697-45705 (2003).
64. Hoffman, M.P., Engbring, J.A., Nielsen, P.K., Vargas, J., Steinberg, Z., Karmand, A.J., Nomizu, M., Yamada, Y., Kleinman, H.K., *J. Biol. Chem.*, **276**, 22077–22085 (2001).

65. Rodin, S., Domogatskaya, A., Ström, S., Hansson, E.M., Chien, K.R., Inzunza, J., Hovatta, O., Tryggvason, K., *Nat. Biotechnol.*, **28**, 611–615 (2010).
66. Katagiri, F., Ishikawa, M., Yamada, Y., Hozumi, K., Kikawa, Y., Nomizu, M., *Arch Biochem Biophys.*, **521**, 32–42 (2012).
67. Yamada, Y.; Onda, T.; Hamada, K.; Kikkawa, Y.; Nomizu, M. *Biol. Pharm. Bull.*, **45**, 207-212 (2022).
68. Chia, J.Y.; Miki, T.; Mihara, H.; Tsutsumi, H., *Bioorg. Med. Chem.* **46**, 116345 (2021).

LIST OF PUBLICATIONS

This list is up to date at the present time (January 2023)

Publications in journals as research papers:

1. Guangrui Zhang, Yuji Yamada, Jun Kumai, Keisuke Hamada, Yamato Kikkawa, Motoyoshi Nomizu, Structural Requirement of hA5G18 Peptide (DDFVFYVGGYPS) from Laminin α5 Chain for Amyloid-like Fibril Formation and Cell Adhesion, *Molecules.*, **27(19)**, 6610 (2022).

ACKNOWLEDGEMENTS

I would like to thank a number of people for their guidance and support throughout my Ph.D. career here at the Tokyo University of Pharmacy and Life Sciences. First, I feel truly honored to have had Prof. Motoyoshi Nomizu as an adviser and mentor. You are a very caring person who is always concerned with your student and their family's well-being. I deeply appreciate your high standards for group meeting presentations, conferences, and publications. Thank you for everything you have done to get me where I am. Your pioneering spirit, creative mind, and love for science are qualities I hope to possess for the rest of my life.

All the past and present members of Nomizu's lab have been like a second family to me in Japan. It is hard to believe I've already lived in this lovely place for six years. Our heated scientific argument and controversial research topics contributed to unforgettable memory in my Ph.D. Thanks to Dr. Yuji Yamada and Dr. Keisuke Hamada for mentoring and guiding me throughout the years. and thanks to Dr. Yamato kikkawa and Dr. Kentaro Hozumi introduced me to the wonderful world of peptide chemistry. They gave me much practical advice and help from the start.

My family has been a source of never-ending and unconditional support. Mr. Yumin Zhang and Ms. Lu Yuan have been absolutely incredible. Thanks to them for giving me the confidence to keep going every time I fail in the experiment. And for my friends Ms. Fan Yang, Mr. Yi Yang, Mr. Chenguang Zhou and Ms. Shuaiyi Li, I have to say thank you for your guys accompanying me through the tough times in the last four years.